INTERNATIONAL ATOMIC ENERGY AGENCY
UNITED NATIONS EDUCATIONAL, SCIENTIFIC AND CULTURAL O NIZATION
INTERNATIONAL CENTRE FOR THEORETICAL HYSICS
I.C.T.P., P.O. BOX 586, 34100 TRIESTE, ITALY, CABLE: CENTRAT TRIESTE

H4.SMR/845-1

Second Winter College on Optics

20 February - 10 March 1995

Basics of Holography

P. Hariharan

CSIRO Division of Applied Physics
Sydney, Australia

Basics of Holography

P. Hariharan

CSIRO Division of Applied Physics, Sydney,

Australia

Contents

1. Introduction 1

2. The development of holography 3

3. Off-axis holograms 7

3.1 Reflection holograms 9

3.2 Image holograms 11

4. The reconstructed image 13

5. Image speckle 17

5.1 Signal-to-noise ratio 19

6. Types of holograms 21

6.1 Thin amplitude and phase gratings 21

6.2 Volume gratings 23

6.3 Thin gratings and volume gratings 27

6.4 Holograms of diffusely reflecting objects 29

6.5 Multiply exposed holograms 29

7. Light sources 33

7.1 Coherence requirements 33

7.2 Laser beam expansion 35

7.3 Beam polarization 37

7.4 Holography with pulsed lasers 38

7.5 Laser safety 38

8. Recording media 41

8.1 Effects of nonlinearity 41

9. Practical recording materials 47

9.1 Photographic materials 47

9.2 Dichromated gelatin 48

9.3 Photoresists 49

9.4 Photopolymers 51

9.5 Photothermoplastics 51

9.6 Photorefractive crystals 53

10. Display holograms 57

10.1 Reflection holograms 57

10.2 Rainbow holograms 59

10.3 Holographic stereograms 63

10.4 Multicolour holograms 65

11. Particle imaging 71

12. Holographic optical elements 77

12.1 Diffraction gratings 77

12.2 Holographic scanners 78

12.3 Aberration correction 79

12.4 Head-up displays 79

12.5 Multiple imaging 80

12.6 Interconnections 83

13. Holographic interferometry 85

13.1 Real-time holographic interferometry 85

13.2 Double-exposure holographic interferometry 88

13.3 Phase difference in the interference pattern 91

13.4 The holodiagram 92

13.5 Fringe localization 92

13.6 Stroboscopic holographic interferometry 93

13.7 Time-average holographic interferometry 94

1 Introduction

This tutorial is intended as an introduction to the subject of holography and will discuss its theory and practice, as well as some of its important applications.

In the first part, after a brief historical retrospect, we will review image formation by a hologram, the characteristics of the reconstructed image, and the basic types of holograms. This will be followed by a discussion of light sources and optical systems used for holography, and hologram recording media and their characteristics. Finally, we will describe methods for the production of different types of holograms for displays, as well as some of the most important technical applications of holography, such as particle imaging, holographic optical elements and holographic interferometry.

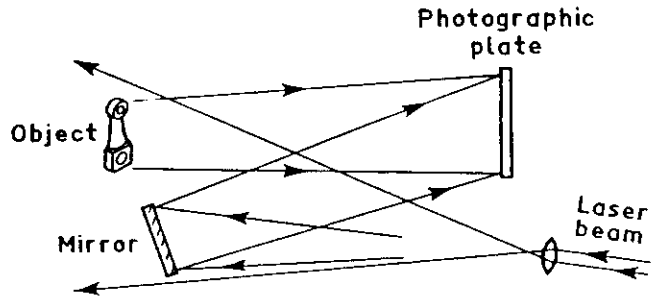

Fig. 2.1 Hologram recording: the interference pattern produced by the reference wave and the object wave is recorded

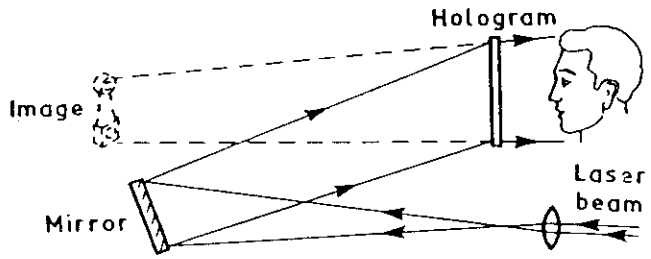

Fig. 2.2 Image reconstruction: light diffracted by the hologram recreates the object wave

2 The development of holography

The unique characteristic of holography is its ability to record both the phase and the amplitude of the light waves from an object. This is not possible with conventional imaging techniques, since all recording materials respond only to the intensity. Holography gets around this problem by using coherent illumination and introducing, as shown in Fig. 2.1, a reference beam derived from the same source. The photographic film records the interference pattern produced by this reference beam and the light waves scattered by the object.

The resulting recording (the hologram) contains information on the phase as well as the amplitude of the object wave, since the intensity at any point in this interference pattern depends on the phase as well as the amplitude of the object wave. If the hologram is illuminated once again with the original reference wave, as shown in Fig. 2.2, it reconstructs the object wave. An observer looking through the hologram sees a perfect three-dimensional image of the object.

In Gabor's historical demonstration of holographic imaging [2.1], a transparency consisting of opaque lines on a clear background was illuminated with a collimated beam of monochromatic light, and the interference pattern produced by the directly transmitted beam (the reference wave) and the light scattered by the lines on the transparency was recorded on a photographic plate. When the hologram (a positive

transparency made from this plate) was illuminated with the original collimated beam, it produced two diffracted waves, one reconstructing an image of the object in its original location, and the other, with the same amplitude but opposite phase, forming a second, conjugate image. However, a major drawback was that the conjugate image, as well as scattered light from the directly transmitted beam, seriously degraded the reconstructed image.

The twin-image problem was finally solved when Leith and Upatnieks [2.2-2.4] developed the off-axis reference beam technique, already shown schematically in Figs. 2.1 and 2.2. This technique used a separate reference wave incident on the photographic plate at an appreciable angle to the object wave. As a result, when the hologram was illuminated with the original reference beam, the two images were separated by large enough angles from the directly transmitted beam and from each other to ensure that they did not overlap.

The development of the off-axis technique resulted in a surge in activity in holography, and led in due course to several important applications.

References

2.1 D. Gabor: Nature, 161, 777-778 (1948)

2.2 E. N. Leith, J. Upatnieks: J. Opt. Soc. Am. 52, 1123-1130 (1962)

2.3 E. N. Leith, J. Upatnieks: J. Opt. Soc. Am. 53, 1377-1381 (1963)

2.4 E. N. Leith, J. Upatnieks: J. Opt. Soc. Am. 54, 1295-1301 (1964)

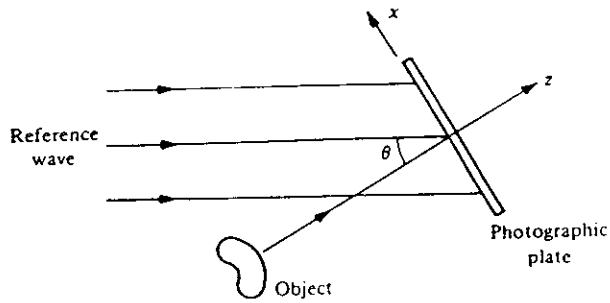

Fig. 3.1 The off-axis hologram: recording setup

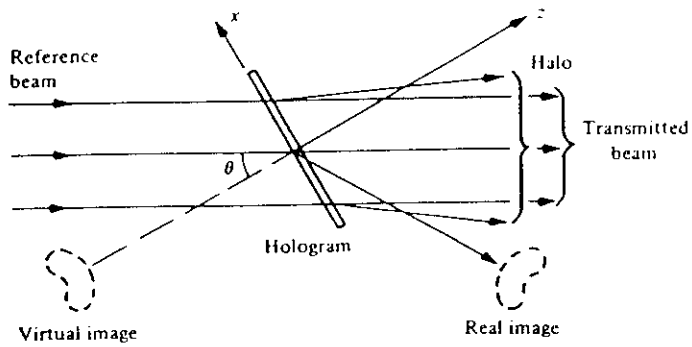

Fig. 3.2 The off-axis hologram: image reconstruction

3 Off-axis holograms

We will now discuss the formation of an image by an off-axis hologram in more detail. We consider, for simplicity, the recording arrangement shown in Fig. 3.1, in which the reference beam is a collimated beam of uniform intensity, derived from the same source as that used to illuminate the object.

The complex amplitude at any point (x,y) on the photographic plate due to the reference beam can then be written as

$$r(x,y) = r \exp(i2\pi\xi x), \tag{3.01}$$

where $\xi = (\sin \theta)/\lambda$, since only its phase varies across the photographic plate, while that due to the object beam, for which both the amplitude and phase vary, can be written as

$$o(x,y) = |o(x,y)| \exp [-i\varphi(x,y)]. \tag{3.02}$$

The resultant intensity is, therefore,

$$\begin{aligned} I(x,y) &= |r(x,y) + o(x,y)|^2 \\ &= |r(x,y)|^2 + |o(x,y)|^2 \\ &\quad + r|o(x,y)| \exp[-i\varphi(x,y)] \exp(-i2\pi\xi x) \\ &\quad + r|o(x,y)| \exp[i\varphi(x,y)] \exp(i2\pi\xi x) \end{aligned}$$

$$= r^2 + |o(x,y)|^2 + 2r|o(x,y)| \cos[2\pi\xi x + \varphi(x,y)]. \qquad (3.03)$$

For simplicity, we can assume that the amplitude transmittance of the photographic plate is a linear function of the intensity and is given by the relation

$$t = t_0 + \beta T I, \qquad (3.04)$$

where t_0 is a constant background transmittance, T is the exposure time and β is the slope (negative) of the amplitude transmittance *vs* exposure characteristic of the photographic plate. The resultant amplitude transmittance of the hologram is then

$$\begin{aligned} t(x,y) = t_0 + \beta T\{&|o(x,y)|^2 \\ &+ r|o(x,y)| \exp[-i\varphi(x,y)] \exp(-i2\pi\xi x) \\ &+ r|o(x,y)| \exp[i\varphi(x,y)] \exp(i2\pi\xi x)\}. \end{aligned} \qquad (3.05)$$

When the hologram is illuminated once again with the same reference beam, as shown schematically in Fig. 3.2, the complex amplitude of the transmitted wave can be written as

$$\begin{aligned} u(x,y) &= r(x,y)\ t(x,y) \\ &= t_0 r \exp(i2\pi\xi x) + \beta T r\ |o(x,y)|^2 \exp(i2\pi\xi x) \\ &\quad + \beta T r^2 o(x,y) + \beta T r^2 o^*(x,y) \exp(i4\pi\xi x). \end{aligned} \qquad (3.06)$$

The first term on the right hand side of Eq. (3.06) is the directly transmitted beam, while the second term yields a halo surrounding it, with approximately twice the angular spread of the object. The third term is identical to the original object wave, except for a constant factor βTr^2, and produces a virtual image of the object in its original position. The fourth term corresponds to the conjugate image, which, in this case is a real image. If the offset angle of the reference beam is made large enough, the virtual image cam be separated from the directly transmitted beam and the conjugate image.

In this arrangement, corresponding points on the real and virtual images are located at equal distances from the hologram, but on opposite sides of it. Since the depth of the real image is inverted, it is called a pseudoscopic image, as opposed to the normal, or orthoscopic virtual image. It should also be noted that the sign of β only affects the phase of the reconstructed image, so that a 'positive' image is always obtained, even if the hologram recording is a photographic negative.

3.1 Reflection holograms

If the object and reference beams are incident on the photographic plate from opposite sides, the interference fringes produced are actually layers within the thickness of the emulsion, about half a wavelength apart [3.1] A hologram recorded in this manner, when

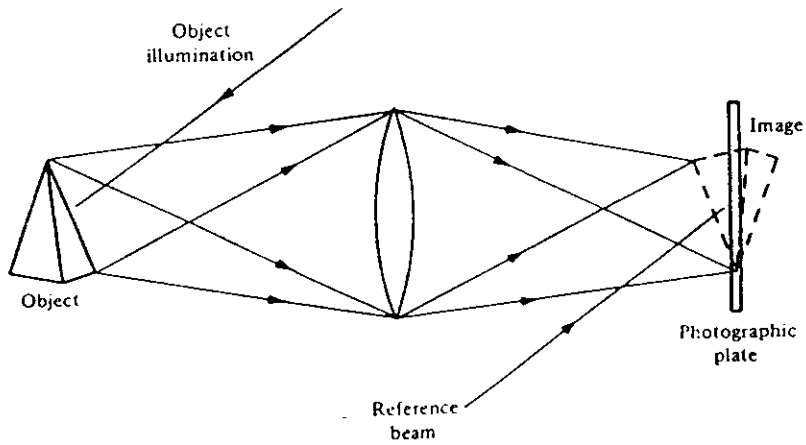

Fig. 3.3 Recording an image hologram

illuminated with a point source of white light, can reconstruct a monochromatic image in reflected light.

3.2 Image holograms

For some applications, there are advantages in recording a hologram of an image of the object formed by a lens. As shown in Fig. 3.3, the hologram plate is set in the central plane of the image, and a hologram is recorded in the normal fashion with an off-axis reference beam. When the hologram is illuminated with the original reference beam, part of the image lies in front of the hologram, and part of the image lies behind it. Since the image is very close to the hologram plane, it is possible to relax the spatial and temporal coherence requirements for the illumination used to reconstruct the image [3.2].

References

3.1 Yu. N. Denisyuk, Soviet Physics - Doklady, 7, 543-545 (1962).

3.2 L. Rosen: Appl. Phys. Lett. 9, 337-339 (1966)

Problems

3.1. A transmission hologram is recorded using a He-Ne laser (λ = 633 nm) with the object and reference beams making angles of $+30^{o}$ and -30^{o}.

respectively, with the normal to the photographic plate. What is the average spatial frequency of the hologram fringes?

The average spatial frequency of the hologram fringes is

$$\xi = 2 \sin 30^{o} / 633 \times 10^{-9} \ m^{-1}$$
$$= 1579 \text{ lines/mm.}$$

3.2. What would be the spatial frequency of the fringes in a reflection hologram if the object beam is normal to the photographic plate and the reference beam makes an angle of 45^{o} with the normal?

The wavelength of the laser in the unexposed photographic emulsion (refractive index 1.6) is 633 / 1.6 = 395.6 nm. The reference beam, after refraction, makes an angle of 26.3^{o} with the normal, so that the two beams make angles of $\pm$ 76.85^{o} with the fringe planes. The spatial frequency of the fringes is, therefore,

$$\xi = 2 \sin 76.85^{o} / 395.6 \times 10^{-9} \ m^{-1}$$
$$= 4923 \text{ lines/mm.}$$

4. The reconstructed image

To study the characteristics of the reconstructed image and their dependence on the optical system, we consider, as shown in Fig. 4.1, the hologram of a point object $O(x_0,y_0,z_0)$, recorded with a reference wave from a point source $R(x_R,y_R,z_R)$, using light of wavelength λ_1. If the hologram is illuminated with monochromatic light of wavelength λ_2 from a point source $P(x_p,y_p,x_p)$, it can be shown that the coordinates of the image of O are [4.1]

$$x_I = \frac{x_P z_0 z_R + \mu x_0 z_P z - \mu x_R z_P z_0}{z_0 z_R + \mu z_P z_R - \mu z_P z_0}. \qquad (4.01)$$

$$y_I = \frac{y_P z_0 z_R + \mu y_0 z_P z_R - \mu y_R z_P z_0}{z_0 z_R + \mu z_P z_R - \mu z_P z_0}. \qquad (4.02)$$

$$z_I = \frac{z_P z_0 z_R}{z_0 z_R + \mu z_P z_R - \mu z_P z_0}, \qquad (4.03)$$

where $\mu = (\lambda_2/\lambda_1)$. The lateral magnification of the image can be defined as

$$M_{lat} = (dx_I/dx_0) = (dy_I/dy_0)$$

$$= 1 \Big/ \left[1 + z_0\left[\frac{1}{\mu z_P} - \frac{1}{z_R}\right]\right]. \qquad (4.04)$$

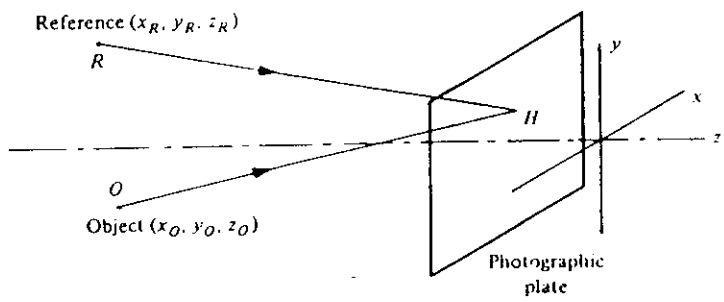

Fig. 4.1 Formation of the image of a point object

If the hologram is illuminated with the same reference wave used to record it, the image has the same size as the original object and coincides with it. However, any change in the position or the wavelength of the point source used for reconstruction results in a change in the position and magnification of the reconstructed image.

References

4.1 R. W. Meier: J. Opt. Soc. Am. 55, 987-992 (1965)

Problems

4.1. A hologram is recorded using a pulsed ruby laser (λ = 694 nm), and illuminated with a He-Ne laser (λ = 633 nm) to view the image. The reference beam in the recording system appears to diverge from a point at a distance of 1 m from the hologram. How far from the hologram should the beam from the He-Ne laser be brought to a focus to ensure that the image is reconstructed with unit magnification?

From Eq. (4.04) it follows that the condition for the image to be reconstructed with unit magnification is

$$\mu z_P = z_R$$

where z_P and z_R are the distances of the source used for reconstruction and recording, respectively, from the hologram, and μ is the ratio of their wavelengths. Accordingly, the beam from the He-Ne laser should be brought to a focus at a distance from the hologram

$$z_P = 1 \times 694 / 633$$
$$= 1.096 \text{ m.}$$

5. Image speckle

When a diffusely reflecting object is illuminated, each element on its surface produces a diffracted wave. With coherent light, these diffracted waves can interfere with each other. Since the optical paths to neighboring elements may differ by several wavelengths, local fluctuations are seen in the intensity in the far field. As a result, the image exhibits a speckled appearance. With polarized light, the intensity in the speckle pattern has, as shown in Fig. 5.1, the negative exponential distribution

$$p(I) = (1/2\sigma^2) \exp(-I/2\sigma^2), \tag{5.01}$$

where $2\sigma^2$ is the mean intensity [5.1]. The contrast of the speckle pattern is unity, and its appearance is almost independent of the nature of the surface, but the size of the speckles increases with the viewing distance and the f-number of the imaging system. With a circular pupil of radius ρ, the average size of the speckles in the image is

$$\Delta x = \Delta y = 0.61\, \lambda f/\rho. \tag{5.02}$$

Speckle is a serious problem in holographic imaging. While several techniques have been described to reduce speckle in the reconstructed image [5.2], the most common method is to record a number of holograms with the object illuminated from slightly different directions. Each of

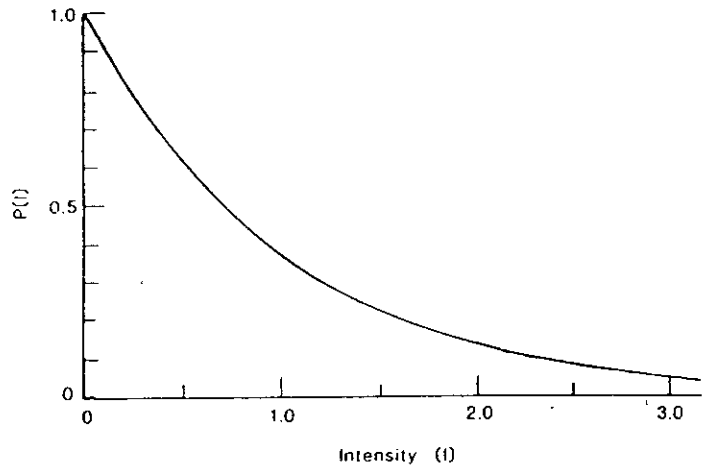

Fig. 5.1 Intensity distribution in a speckle pattern

these holograms reconstructs the same image, but a different speckle pattern. If the images produced by N such holograms are superposed, the contrast in the speckle pattern is reduced by a factor equal to $\sqrt{N}$.

5.1 Signal-to-noise ratio

Random spatial variations in the intensity of the reconstructed image, commonly caused by scattered light, are referred to as noise. However, when calculating the signal-to-noise ratio, the amplitudes of the signal and the noise must be added, since they are both encoded on a common carrier [5.3].

We consider the reconstructed image of a uniform bright patch on a dark background, and assume that the intensity due to the nominally uniform signal is I_S, while that of the randomly varying background is I_N. The noise N in the bright area is given by the variance of the resulting fluctuations of the intensity. It can then be shown that when $I_S \gg \langle I_N \rangle$, as is usually the case, the signal-to-noise ratio is

$$I_S / N = (I_S / 2\langle I_N \rangle)^{\frac{1}{2}}. \qquad (5.03)$$

Even a small amount of scattered light can result in relatively large fluctuations in intensity in the bright areas of the image.

References

5.1 J. W. Goodman: "Statistical Properties of Laser Speckle Patterns", in *Laser Speckle and Related Phenomena*, ed. by J. C. Dainty, Topics. Appl. Phys. , Vol. 9 (Springer, Berlin 1975) pp. 9–75

5.2 T. S. McKechnie: "Speckle Reduction", in *Laser Speckle and Related Phenomena*, ed. by J. C. Dainty, Topics. Appl. Phys. , Vol. 9 (Springer, Berlin 1975) pp. 123–170

5.3 J. W. Goodman: J. Opt. Soc. Am. 57, 493–502 (1967)

Problems

5.1. The image reconstructed by a hologram illuminated with a He-Ne laser (λ = 633 nm) is to be photographed using a camera with a lens having a focal length of 100 mm, stopped down to get the maximum depth of focus in the image. What is the minimum aperture that can be used for the speckle size in the image to be less than 0.01 mm.

From Eq. (5.02), the minimum radius of the lens aperture is

$$\rho_{min} = 0.61 \times 633 \times 10^{-9} \times 100 \times 10^{-3} / 0.01 \times 10^{-3} \text{ m}$$
$$= 3.86 \text{ mm},$$

which would correspond to an f-number of 100 / 3.86 × 2 = 12.95.

6. Types of holograms

So far, we have treated a hologram recorded on a photographic film as equivalent, to a first approximation, to a grating of negligible thickness with a spatially varying transmittance. However, with modified processing techniques, or with other recording materials, it is possible to reproduce the variations in the intensity in the interference pattern produced by the object and reference beams as variations in the refractive index, or the thickness, of the hologram. Accordingly, holograms can be classified, in the first instance as amplitude and phase holograms.

In addition, if the thickness of the recording medium is much larger than the average spacing of the fringes, volume effects cannot be neglected. It is even possible to produce holograms, in which the interference pattern consists of planes running almost parallel to the surface of the recording material, that reconstruct an image in reflected light. Holograms recorded in thick media can therefore be subdivided into volume transmission holograms and volume reflection holograms.

6.1 Thin amplitude and phase gratings

The amplitude transmittance of a thin amplitude grating can be written as

$$t(x) = t_0 + \Delta t \cos Kx, \tag{6.01}$$

where t_0 is the average amplitude transmittance, Δt is the amplitude of the spatial variations of $t(x)$, and $K = 2\pi/\Lambda$, where Λ is the average spacing of the fringes. The maximum amplitude in each of the two diffracted orders is a fourth of that in the incident wave, so that the maximum diffraction efficiency is

$$\eta_{max} = 0.0625. \tag{6.02}$$

If the phase shift produced by the recording medium is proportional to the intensity in the interference pattern, the complex amplitude transmittance of a thin phase grating can be written as

$$t(x) = \exp(-i\varphi_0)\, \exp[-i\Delta\varphi \cos(Kx)], \tag{6.03}$$

where φ_0 is a constant phase factor, and $\Delta\varphi$ is the amplitude of the phase variations. If we neglect this constant phase factor, the right hand side of Eq. (6.03) can be expanded to obtain the relation [6.1]

$$t(x) = \sum_{n=-\infty}^{\infty} i^n J_n(\Delta\varphi) \exp(inKx), \tag{6.04}$$

where J_n is the Bessel function of the first kind, of order n.

Equation (6.04) shows that the incident beam is diffracted into a number of orders, with the diffracted amplitude in the nth order proportional to the value of the Bessel function $J_n(\Delta\varphi)$. Only the first order contributes to the image reconstructed by a hologram. The diffraction efficiency of the phase grating can therefore be written as

$$\eta = J_1^2(\Delta\varphi). \tag{6.05}$$

As shown in Fig. 6.1, the diffraction efficiency of a thin phase grating increases initially with the phase modulation and then decreases; its maximum value is

$$\eta_{max} = 0.339. \tag{6.06}$$

6.2 Volume gratings

With a thick recording medium, the hologram is made up of layers corresponding to a periodic variation of transmittance or refractive index. If the two interfering wavefronts are incident on the recording medium from the same side, these layers are approximately perpendicular to its surface, and the hologram produces an image by transmission. However, it is also possible to have the two interfering wavefronts incident on the recording medium from opposite sides, in which case the interference surfaces run approximately parallel to the surface of the recording medium. In this case, the reconstructed image is produced by

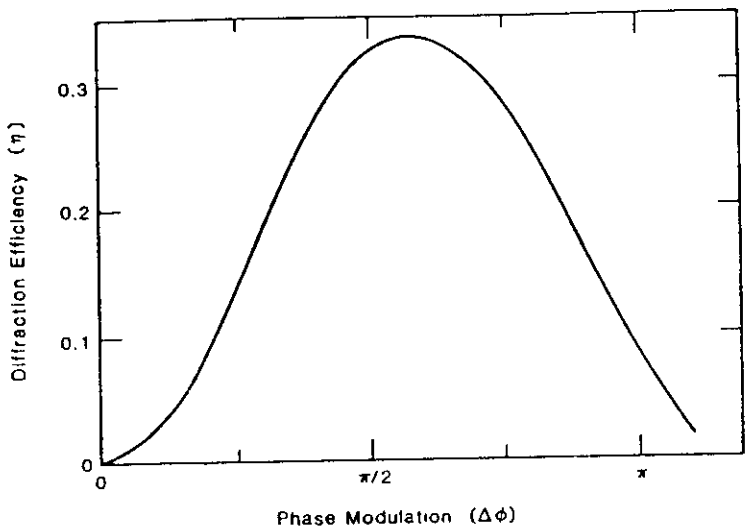

Fig. 6.1 Diffraction efficiency of a thin phase grating as a function of the phase modulation

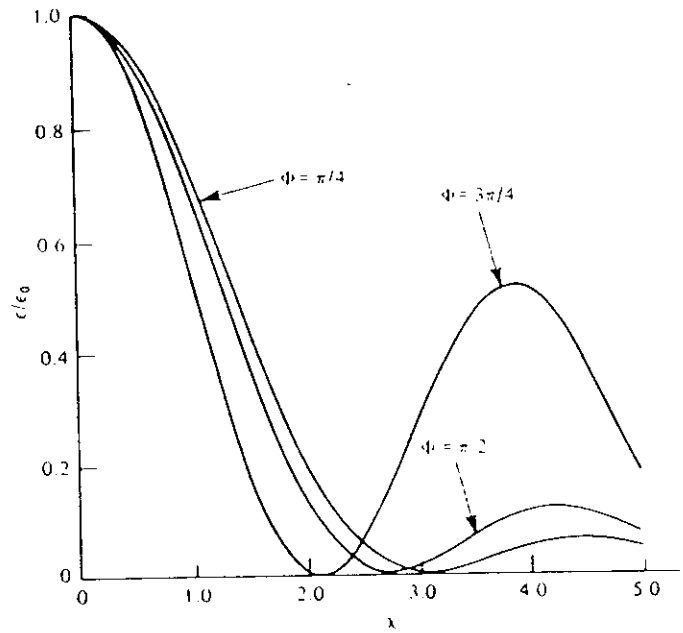

Fig. 6.2 Normalized diffraction efficiency of a volume phase transmission grating as a function of the deviation from the Bragg condition [Kogelnik, 1969]

the light reflected from the hologram. In both cases, the diffracted amplitude is a maximum only when the Bragg condition is satisfied. With volume reflection holograms, the angular and wavelength selectivity can be high enough to produce an image with white light. As a result, volume reflection holograms are used widely in displays.

When analyzing the diffraction of light by volume gratings, it is necessary to take into account the fact that the amplitude of the diffracted wave increases progressively, while that of the incident wave decreases, as they propagate through the grating. This problem was solved by the development of a coupled wave theory [6.1, 6.2]. Some of the most important results for volume transmission gratings are summarized below.

6.2.1 Volume transmission gratings

We consider, in the first instance, a lossless, volume transmission phase grating of thickness d, with the grating planes running normal to its surface. If we assume that the refractive index varies sinusoidally, with an amplitude Δn, about a mean value n, the diffraction efficiency of the grating at the Bragg angle θ_B is

$$\eta_B = \sin^2 \Phi, \qquad (6.07)$$

where $\Phi = \pi \Delta n\, d/\lambda \cos \theta_B$, is known as the modulation parameter. The

diffraction efficiency increases initially as the modulation parameter Φ is increased, until, when $\Phi = \pi/2$, $\eta_B = 1$. Beyond this point, the diffraction efficiency decreases.

For a deviation $\Delta\theta$ in the angle of incidence from the Bragg angle, the diffraction efficiency drops to

$$\eta = \frac{\sin^2 (\Phi^2 + \chi^2)^{\frac{1}{2}}}{(1 + \chi^2/\Phi^2)}, \qquad (6.08)$$

where

$$\chi = \Delta\theta.\mathrm{Kd}/2. \qquad (6.09).$$

Figure 6.2 shows the normalized diffraction efficiency as a function of the parameter χ, for three values of the modulation parameter Φ.

The other case we shall consider is that of a volume transmission grating in which the refractive index does not vary, but the absorption constant varies with an amplitude $\Delta\alpha$ about its mean value α. In this case, the diffraction efficiency is given by the expression

$$\eta = \exp (-2\alpha d/\cos \theta_B) \sinh^2 (\Delta\alpha \, d/2 \cos \theta_B) \qquad (6.10)$$

The maximum diffraction efficiency is obtained when

$$\Delta\alpha = \alpha = (\ln 3)/\, d \cos \theta_B \qquad (6.11)$$

and has a value $\eta_{max} = 0.037$.

6.2.2 Volume reflection gratings

The diffraction efficiency of a volume phase reflection grating at the Bragg angle is given by the relation

$$\eta_B = \tanh^2 \Phi_R \qquad (6.12)$$

where $\Phi_R = \pi n_1 d/\lambda \cos \theta_B$. As the value of Φ_R increases, the diffraction efficiency increases to a limiting value of 1.00.

The diffraction efficiency drops to zero for a deviation from the Bragg condition $\chi_R \approx 3.5$, where

$$\chi_R = \Delta\theta\, (2\pi n_0 d/\lambda) \sin \theta_B$$
$$= (\Delta\lambda/\lambda)(2\pi n_0 d/\lambda) \cos \theta_B. \qquad (6.14)$$

6.3 Thin gratings and volume gratings

The distinction between thin gratings and volume gratings is commonly made [6.3] on the basis of a parameter Q defined by the relation

Table 6.1 Maximum theoretical diffraction efficiencies for transmission phase holograms

Type of hologram	Thin		Volume	
Object beam	Collimated	Diffuse	Collimated	Diffuse
η_{max}	0.33	0.22	1.00	0.64

$$Q = 2\pi\lambda d/n\Lambda^2 . \qquad (6.15)$$

Small values of Q (Q<1) correspond to thin gratings, while large values of Q (Q>1) correspond to volume gratings. However, more detailed studies have shown that the transition between the two regimes is not completely defined by Eq. (6.15) and that, as the modulation amplitude increases, an intermediate regime appears and widens [6.4, 6.5].

6.4 Holograms of diffusely reflecting objects

The values of diffraction efficiency obtained with a hologram of a diffusely reflecting object are always much lower than those for a grating, because it is not possible to maintain optimum modulation over the entire area, due to the nonuniformity of the object wave. The maximum diffraction efficiencies of transmission phase holograms recorded with a diffuse object beam have been calculated [6.6], on the assumption that the amplitude of the object wave has similar statistics to a speckle pattern, and are presented in Table 6.1.

6.4 Multiply exposed holograms

With a thick recording medium, it is possible to record two or more holograms in the same medium and read them out separately. In order to do this, the Bragg angles should be sufficiently far apart that the maximum of the angular selectivity curve for one hologram coincides with

the first minimum for the other. However, with N amplitude transmission holograms, the diffraction efficiency of each hologram drops to $1/N^2$ of that for a single hologram, since the available dynamic range is divided equally between the N holograms [6.7].

On the other hand, with volume phase holograms whose Bragg angles are far enough apart for coupling between the gratings to be negligible, each hologram diffracts independently of the others [6.8]. However, if the recording medium is nearing saturation, the consequent reduction in modulation can result in a decrease in the diffraction efficiencies of the individual holograms.

References

6.1 H. Kogelnik: Bell Syst. Tech. J. **48**, 2909-2947 (1969)

6.2 L. Solymar, D. J. Cooke: *Volume Holography and Volume Gratings* (Academic Press, New York 1981) pp. 164-253

6.3 W.R Klein, B. D. Cook: IEEE Trans. Sonics & Ultrasonics, **SU-14**, 123-134 (1967)

6.4 M. Moharam, T. K. Gaylord, R. Magnusson: Opt. Commun. **32**, 14-18 (1980)

6.5 M. Moharam, T. K. Gaylord, R. Magnusson: Opt. Commun. **32**, 19-23 (1980)

6.6 J. Upatnieks, C. Leonard: J. Opt. Soc. Am. **60**, 297-305 (1970)

6.7 R. J. Collier, C. B. Burckhardt, L. H. Lin: *Optical Holography* (Academic Press, New York 1971) pp. 520-521

6.8 S. K. Case, J. Opt. Soc. Am. 65, 724-729 (1975)

Problems

6.1 A volume transmission phase grating (spatial frequency 1579 lines/mm) recorded in a gelatin layer with a thickness of 15 μm, has a diffraction efficiency of 100 percent at the Bragg angle. What would be the angular selectivity of the grating at a wavelength of 633 nm?

The spacing of the grating fringes is $\Lambda = 0.633$ μm, so that the value of the grating vector $K = 2\pi / \Lambda = 9.926 \times 10^6$ m^{-1}. Since the diffraction efficiency of the grating at the Bragg angle is 100 percent, the modulation parameter $\Phi = \pi/2$. From the curve in Fig. 6.2 corresponding to this value of Φ, the diffraction efficiency of the grating drops to zero when the dephasing parameter $\chi = 2.7$. Accordingly, from Eq. (6.09), the deviation from the Bragg angle (within the gelatin layer) at which the diffraction efficiency drops to zero is

$$\Delta\theta = 2\chi / Kd = 2 \times 2.7 / 9.926 \times 10^6 \times 15 \times 10^{-6}$$
$$= 3.63 \times 10^{-2} \text{ radian}$$
$$= 2.08^{\circ}.$$

6.2 A volume reflection phase grating (see problem 3.2) is recorded in a photographic emulsion layer with a thickness of 15μm. What would be the wavelength selectivity of this grating at a mean wavelength of 633 nm?

Within the emulsion layer, the effective wavelength is 395.6 nm and the Bragg angle is 90- 76.85 = 13.15^{o}. From Eq. (6.14), the diffraction efficiency drops to zero for a change in wavelength

$$\Delta\lambda = 3.5\ (395.6 \times 10^{-9})^2 \ /\ 2\pi \times 1.6 \times 15 \times 10^{-6} \cos 13.15^{o}$$

$$= 3.73 \text{ nm}.$$

7. Light sources

In order to obtain maximum fringe visibility while recording a hologram, it is essential to use coherent illumination. Lasers are therefore employed almost universally as light sources in holography. The characteristics of some of the lasers used for holography are listed in Table 7.1.

7.1 Coherence requirements

Operation of the laser on a single spectral line can be obtained, where necessary, by means of a wavelength selector prism. Spatial coherence is then ensured if the laser oscillates in the lowest order transverse mode (the TEM_{00} mode). However, most lasers will then oscillate, as shown in the top part of Fig. 7.1, in a number of longitudinal modes lying within the gain profile of the active medium, at which the gain is adequate to overcome the cavity losses. These modes correspond to the resonant frequencies of the laser cavity and are separated by a frequency interval

$$\Delta\nu = c/2L \qquad (7.01)$$

where c is the speed of light, and L is the length of the laser cavity. If we assume that the output power is divided equally between N longitudinal modes, the effective coherence length of the output is

Table 7.1 Characteristics of some lasers used for holography

Laser	Output	Wavelength nm	Power
He - Ne	cw	633	2 - 50 mW
Ar^+	cw	514	~ 1 W
		488	~ 1 W
Kr^+	cw	647	500 mW
Ruby	pulsed	694	1 - 10 J
Diode	cw		~ 5 mW
Dye	cw	tunable	~ 200 mW

$$\Delta l = 2L/N. \qquad (7.02)$$

Equation (7.02) shows that the existence of more than one longitudinal mode in the output reduces the coherence length severely. Even if the mean optical paths of the object and reference beams are equalized carefully, severe restrictions are placed on the maximum depth of the object.

Depending on their power, most commercial He-Ne lasers oscillate in between two and five longitudinal modes, and the coherence length of the output is limited to a few centimetres. With high-power Ar^+ and Kr^+ lasers, it is possible to obtain operation in a single longitudinal mode and coherence lengths in excess of a metre by using an intracavity etalon. This etalon is tuned to obtain maximum power output by mounting it in a temperature-controlled oven.

7.2 Laser beam expansion

Since the beam from a laser typically has a diameter of 1-2 mm, low-power microscope objectives are commonly used to expand it to illuminate the object as well as the hologram. However, due to the high coherence of laser light, the expanded beam usually exhibits random diffraction patterns (spatial noise) produced by defects and dust on the optical surfaces in the path of the beam. These can be eliminated by placing a pinhole at the focus of the microscope objective, as shown in

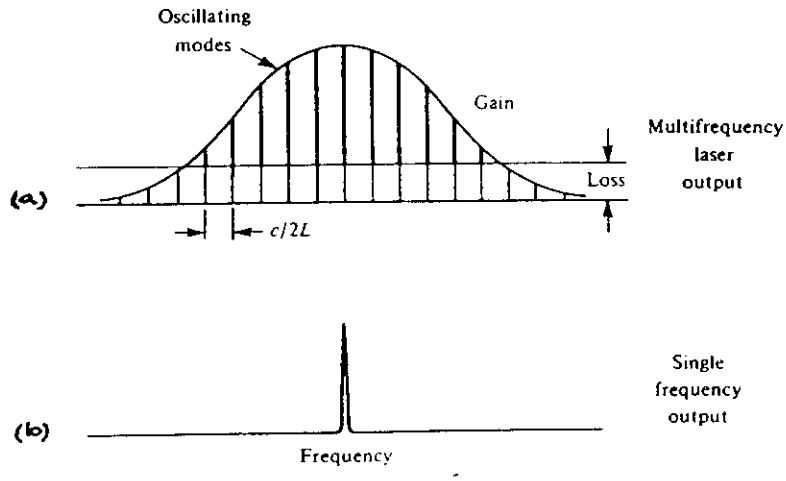

Fig. 7.1 Laser modes: (a) without, and (b) with an intra-cavity etalon

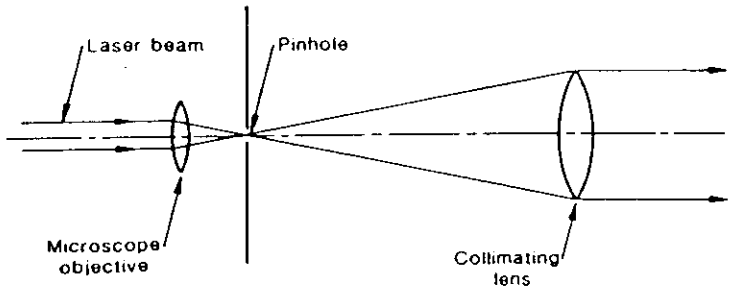

Fig. 7.2 Optical system used to expand and spatially filter a laser beam

Fig. 7.2. If the laser is oscillating in the TEM_{00} mode, the beam has a Gaussian intensity profile given by the relation

$$I(r) = I(0) \exp(-2r^2/w^2), \tag{7.03}$$

where r is the radial distance from the center of the beam and w is the distance at which the intensity drops to $(1/e^2)$ of that at the center of the beam. Usually, the aperture of the microscope objective is greater than 2w; the diameter of the focal spot is then

$$d = 2\lambda f/\pi w, \tag{7.04}$$

where f is the focal length of the microscope objective. With a pinhole whose diameter is less than d, randomly diffracted light is blocked, and the transmitted beam has a smooth profile.

7.3. Beam polarization

The visibility of the interference fringes forming the hologram is a maximum when the electric vectors in the object and reference beams are parallel. This condition is satisfied if the two beams are linearly polarized with their electric vectors normal to the plane containing the beams. If, on the other hand, they are polarized with their electric vectors in the plane containing the beams, the visibility of the

hologram fringes can drop to zero when the beams intersect at right angles.

It should be noted that in the case of an object with a rough surface, a substantial fraction of the reflected light may be depolarized. The resulting decrease in the visibility of the interference fringes can be minimized, where necessary, by using a sheet polarizer in front of the hologram to eliminate the cross-polarized component.

7.4. Holography with pulsed lasers

Very short light pulses (< 20 nanoseconds) can be obtained with a pulsed laser, if a Pockels cell is used as a Q-switch in the laser cavity. As a result, problems of vibration and air currents are largely eliminated, and it is possible to record holograms of transient disturbances. Because their output wavelength is well matched to the peak sensitivity of available photographic materials, and their output energy is fairly large, pulsed ruby lasers are used widely to record holograms in a workshop environment [7.1].

7.5. Laser safety

Since the beam from a laser is focused by the lens of the eye to a very small spot on the retina, direct exposure to low power lasers can

cause eye damage. With pulsed lasers, even stray reflections can be dangerous. It is essential to take all due precautions and, where required, to use appropriate eye protection [7.2].

References

7.1 W. Koechner: "Solid state lasers", in *Handbook of Optical Holography*, ed. by H. J. Caulfield (Academic Press, New York 1979) pp. 257-267

7.2 D. Sliney, M. Wolbarsht: *Safety with Lasers and Other Optical Sources: a Comprehensive Handbook* (Plenum, New York 1980)

PROBLEMS

7.1 A He-Ne laser with a 300 mm long resonant cavity oscillates in two longitudinal modes. What is the coherence length of the radiation?

From Eq. (7.02) the coherence length of the radiation is

$$\Delta l = 2L/N$$
$$= 2 \times 0.3 / 2$$
$$= 0.3 \text{ metre.}$$

7.2 In the arrangement shown in Fig. 7.2, the central part of the beam from a He-Ne laser is isolated by an aperture with a diameter of 2.0 mm

and brought to a focus by a microscope objective with a focal length of 32 mm. What would be a suitable size for the pinhole?

In this case the diameter of the focal spot is equal to the diameter of the Airy disc which is

$$d = 2.44 \times 0.633 \times 10^{-6} \times 32 \times 10^{-3} / 2 \times 10^{-3} \text{ m}$$
$$= 24.4 \ \mu\text{m}$$

A pinhole with a diameter of 20 μm would ensure a clean beam with only a marginal loss of light.

8. Recording media

The response of recording materials used for amplitude holograms can be characterized on a macroscopic scale, as shown in Fig. 8.1, by plotting the resultant amplitude transmittance against the exposure. Similarly, the response of recording materials used for phase holograms can be described, as shown in Fig. 8.2, by a curve showing the effective phase shift as a function of the exposure. However, these curves are not adequate to describe the response of the recording medium on a microscopic scale. This is because the actual intensity distribution to which the material is exposed always differs from that incident on it, due to scattering and absorption in the recording medium. In addition, the response of the material to different spatial frequencies may be affected by the type of processing. Accordingly, it is necessary to specify the response of the material as the spatial frequency s is varied, relative to that at low spatial frequencies ($s \rightarrow 0$), by a parameter $M(s)$, termed the modulation transfer function.

8.1 Effects of nonlinearity

For simplicity, we have assumed so far that the amplitude transmittance of the hologram is a linear function of the intensity as described by Eq. (3.04). However, in practice, this assumption is not always valid. The amplitude transmittance of the processed recording material can then be represented by a polynomial [8.1]

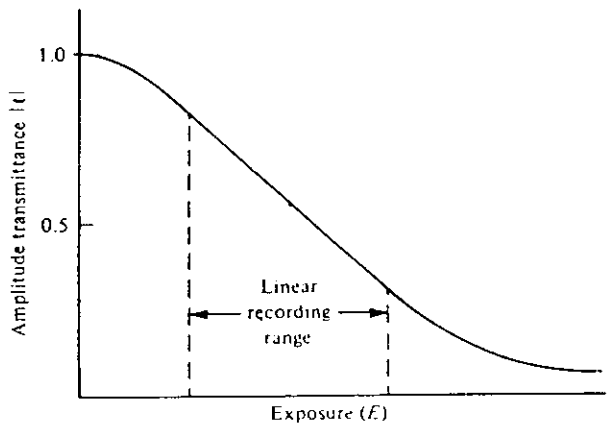

Fig. 8.1 Typical amplitude transmission *vs* exposure curve for a recording material

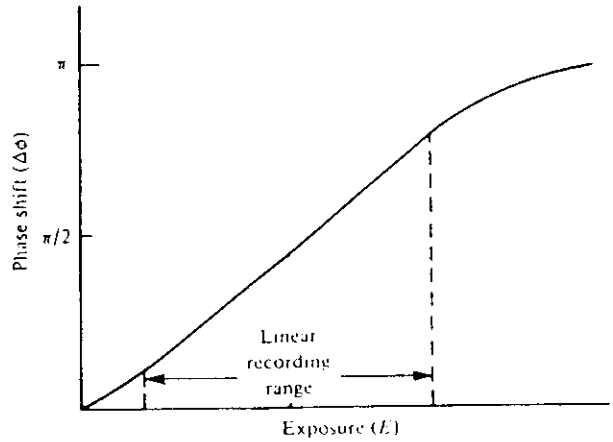

Fig. 8.2 Typical phase-shift *vs* exposure curve for a recording material

$$
\begin{aligned}
t &= t_0 + \beta_1 TI + \beta_2 T^2 I^2 + \ldots \\
&= t_0 + \beta_1 T\,[rr^* + oo^* + r^*o + ro^*] \\
&\quad + \beta_2 T^2 [rr^* + oo^* + r^*o + ro^*]^2 \\
&\quad + \ldots \; .
\end{aligned}
\tag{8.01}
$$

If the hologram is illuminated once again with a plane wave of unit amplitude, the complex amplitude of the wave transmitted by the hologram can be written in the form

$$
\begin{aligned}
u &= \text{linear terms} \\
&\quad + \beta_2 T^2 [(oo^*)^2 + o^2 + o^{*2} + 2o^2 o^* + 2oo^{*2}] \\
&\quad + \ldots \; .
\end{aligned}
\tag{8.02}
$$

Nonlinearity leads, therefore, to the production of additional spurious terms. An examination of Eq. (8.02) shows that the term involving $(oo^*)^2$ results in a doubling of the width of the halo surrounding the directly transmitted beam, while the terms involving o^2 and o^{*2} correspond to higher-order diffracted images, and the terms involving $2o^2o^*$ and $2oo^{*2}$ are intermodulation terms, producing false images.

The effects of nonlinearity are particularly noticeable with phase holograms. Even if we assume that the phase shift produced by the recording medium is proportional to the exposure, the complex amplitude transmittance is given by the expression

$$t = \exp(-i\varphi)$$
$$= 1 - i\varphi - (1/2)\varphi^2 + (1/6)i\varphi^3 \ldots . \qquad (8.03)$$

If the phase modulation is increased to obtain higher diffraction efficiency, the effects of the higher-order terms cannot be neglected.

With volume holograms the effects of nonlinearity are reduced significantly by the angular selectivity of the hologram. If the angle between the beams in the recording setup is large enough that the diffracted beams corresponding to different orders do not overlap, a simple analysis [8.2] shows that the signal-to-noise ratio should improve by a factor approximately equal to $(\psi/\Delta\theta)$, where $2\Delta\theta$ is the width of the passband of the angular selectivity function, and ψ is the angle subtended by the object at the hologram.

References

8.1 O. Bryngdahl, A. Lohmann: J. Opt. Soc. Am. 58, 1325-1334 (1968)

8.2 P. Hariharan: Opt. Acta, 26, 211-215 (1979)

Problem

8.1 A hologram is recorded in an optical system in which the object and reference beams make angles of $+30^{\circ}$ and -30°, respectively with the normal to the photographic plate. After exposure, the plate is

processed to produce a volume phase hologram. If the object subtends an angle of 30^{o} at the photographic plate, and the thickness of the photographic emulsion layer is 15 μm, what is the improvement in the signal-to-noise ratio due to the angular selectivity of the hologram?

Since the modulation parameter for such a hologram would be significantly lower than the optimum value of $\pi/2$ (say $\pi/4$), it follows from Fig. 6.2 that the diffraction efficiency drops to zero when the dephasing parameter $\chi = 3$. From problems 1.1 and 6.1, this would correspond to a deviation from the Bragg angle $\Delta\theta = 2.08^{o}$ within the recording medium, or an angle of about 3.2^{o} in air. The signal-to noise ratio should improve, therefore, by a factor $30/3.2 \approx 9$.

Table 9.1 Recording materials for holography

Material	Exposure J/m^2	Resolution mm^{-1}	Processing	Type of hologram	η_{max} (gratings)
Photo-graphic emulsions	5×10^{-3} to 5×10^{-1}	1000 to 10000	Normal Bleach	Amplitude Phase	0.05 0.60
DCG	10^2	> 10000	Wet	Phase	0.90
Photo-resists	10^2	3000	Wet	Phase	0.30
Photo-polymers	$10-10^4$	5000	Dry	Phase	0.90
Photo-thermo-plastics	10^{-1}	500-1200 (bandpass)	Charge and heat	Thin phase	0.30
BSO	10	> 100000	None	Volume phase	0.20

9 Recording materials

Several recording materials have been used for holography. Table 9.1 lists the principal characteristics of those that have been found most useful.

9.1 Photographic materials

High-resolution photographic plates and films are the most widely used recording materials for holography because of their relatively high sensitivity. Conventional processing produces an amplitude hologram and results in a reduction in the thickness of the emulsion layer of about 15 percent, due to the removal of the unexposed silver halide grains in the fixing bath. This reduction in thickness can cause a rotation of the fringe planes as well as a reduction in their spacing, so that the reference beam is no longer incident on the hologram at the Bragg angle. To minimize the effects of emulsion shrinkage, the object and reference beams should be incident at equal but opposite angles on the hologram, so that the fringe planes are normal to the surface of the photographic emulsion.

Processing can be speeded up and carried out in situ, in a liquid gate, with a monobath in which development and fixing take place simultaneously [9.1]. Higher diffraction efficiencies can be obtained

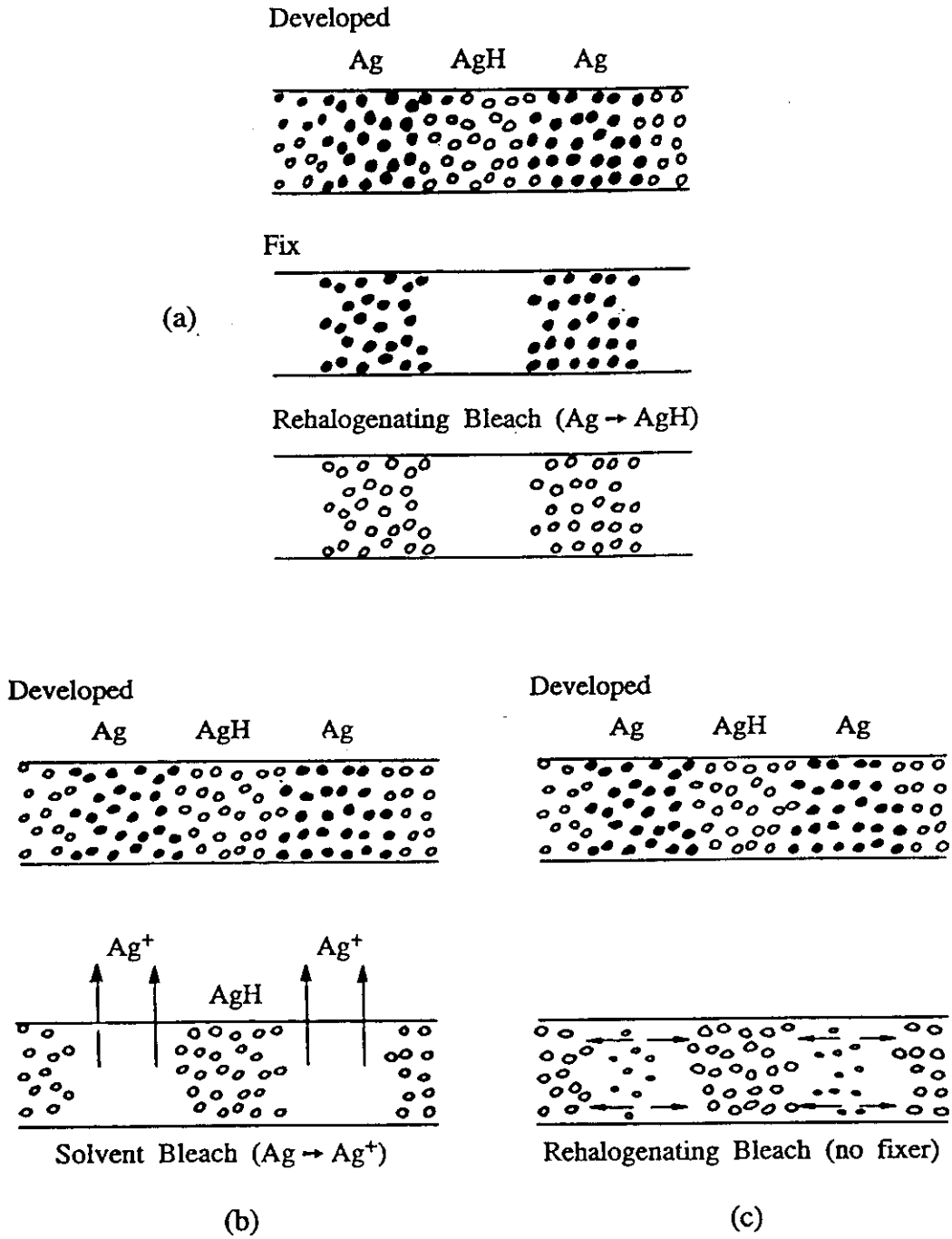

Fig. 9.1 Production of phase holograms by bleaching a photographic material.

by using a bleach bath to convert the developed silver into a transparent silver salt with a high refractive index, as shown in Fig. 9.1, to yield a volume phase hologram [9.2].

9.2 Dichromated gelatin

A gelatin layer containing a small amount of a dichromate, such as $(NH_4)_2Cr_2O_7$, becomes progressively harder on exposure to light, due to the formation of localized cross-links between the carboxylate groups on neighbouring gelatin chains.

After exposure in the holographic system using blue light from an Ar^+ laser (λ = 488 nm), the gelatin layer is washed in water at 20-30^oC for 10 minutes. The gelatin layer absorbs water and swells. The swollen gelatin layer is then immersed in a bath of isopropanol, to extract the water, and dried thoroughly. With care in processing, volume holograms with high diffraction efficiency and low scattering can be produced [9.3].

9.3 Photoresists

In positive photoresists (Shipley AZ-1350), the areas exposed to blue light become soluble and are washed away during development to produce a relief image [9.4]. Such a recording can be replicated, using

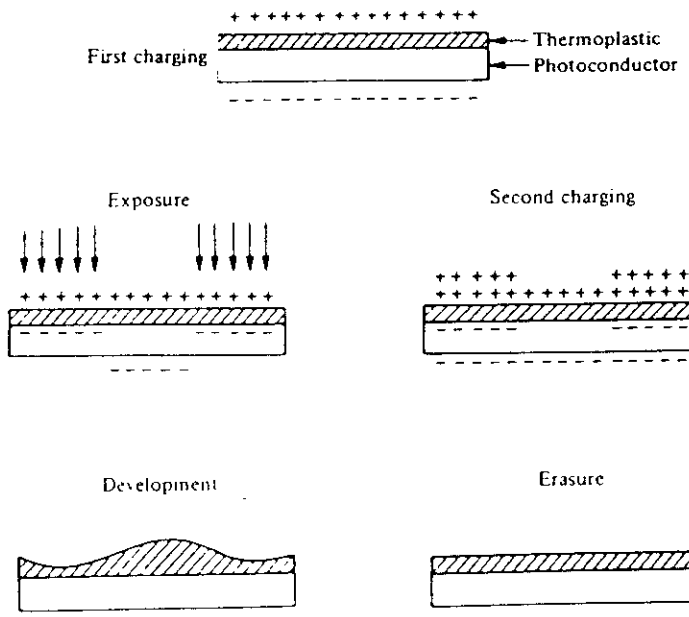

Fig. 9.2 Record-erase cycle for a photothermoplastic [Lin and Beauchamp, 1970]

a thermoplastic, to produce multiple copies of holographic diffraction gratings and holographic optical elements.

9.4 Photopolymers

Several organic materials can be activated by a photo-sensitizer to produce refractive index changes due to photo-polymerization [9.5]. Two commercial photopolymers are available (Polaroid & Du Pont) that can be used to produce volume phase holograms with high diffraction efficiency

9.5 Photothermoplastics

A hologram can also be recorded in a multilayer structure consisting, as shown in Fig. 9.2, of a glass or Mylar substrate coated with a thin, transparent, conducting layer of indium oxide, a photoconductor, and a thermoplastic [9.6]. The film is initially sensitized in darkness by applying a uniform electric charge to the top surface. On exposure and recharging, a spatially varying electrostatic field is created. The thermoplastic is then heated briefly, so that it becomes soft enough to be deformed by this field, and cooled to fix the variations in thickness.

Photothermoplastics have a reasonably high sensitivity and yield a thin phase hologram with good diffraction efficiency. They have the

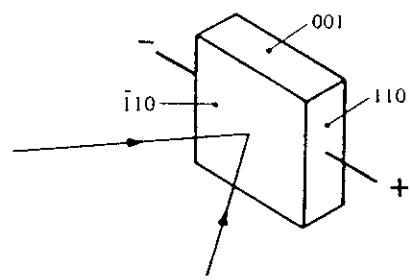

Fig. 9.3 Hologram recording configuration for BSO

advantage that they can be processed rapidly in situ; in addition, if they are produced on a glass substrate, the hologram can be erased by heating the substrate, and the material reused.

9.6 Photorefractive crystals

When a photorefractive crystal is exposed to a spatially varying light pattern, electrons are liberated in the illuminated areas. These electrons migrate to adjacent dark regions and are trapped there. The spatially varying electric field produced by this space-charge pattern modulates the refractive index through the electro-optic effect, producing the equivalent of a phase grating. The space-charge pattern can be erased by uniformly illuminating the crystal, after which another recording can be made.

The photorefractive crystal most commonly used for holographic interferometry has been BSO ($Bi_{12}SiO_{20}$). The best results are obtained with the recording configuration shown in Fig. 9.3, in which an electric field is applied at right angles to the hologram fringes [9.7]. A diffraction efficiency of 0.1 can be obtained with a field of 500 V/mm. Since readout is destructive, the reconstructed image is best recorded and stored for viewing. Several interesting possibilities have been opened up by such photorefractive materials.

References

9.1 P. Hariharan, C. S. Ramanathan, G. S. Kaushik, Appl. Opt. **12**, 611-612 (1973)

9.2 P. Hariharan, J. Phot. Sci. **38**, 76-81 (1990)

9.3 B. J. Chang and C. D. Leonard, Appl. Opt., **18**, 2407-2417 (1979).

9.4 R. A. Bartolini, in *Holographic Recording Materials*, ed. H. M. Smith (Springer-Verlag, Berlin, 1977), pp. 209-227.

9.5 B. L. Booth, J. Appl. Phot. Eng., **3**, 24-30 (1977).

9.6 L. H. Lin and H. L. Beauchamp, Appl. Opt. 9, 2088-2092 (1970)

9.7 J. P. Huignard and F. Micheron, Appl. Phys. Lett. **29**, 591-593 (1976)

Problem

9.1 A hologram is to be recorded with a He-Ne laser on Holotest 8E75 HD plates. The illumination level in the hologram plane due to the object beam is 0.003 W/m^2, and that due to the reference beam is 0.009 W/m^2. Calculate the exposure time required if the plate is to be processed to obtain (a) an amplitude hologram, and (b) a phase hologram.

The appropriate density, after processing, for an amplitude hologram is about 0.7. From the published data for Holotest 8E75 plates, the exposure required for this density is around 0.1 J/m^2, which would correspond to an exposure time of 8 seconds.

For a phase hologram, the exposure should result in a density of about 2.0 after development, which would correspond to an exposure of 0.25 J/m^2, or an exposure time of 20 seconds.

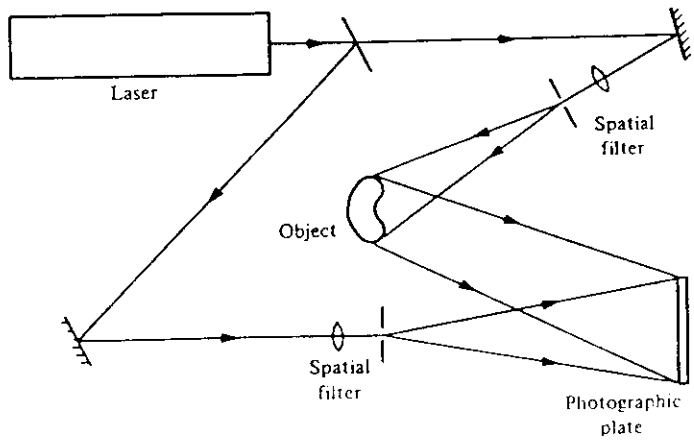

Fig. 10.1 Optical arrangement used to record a transmission hologram

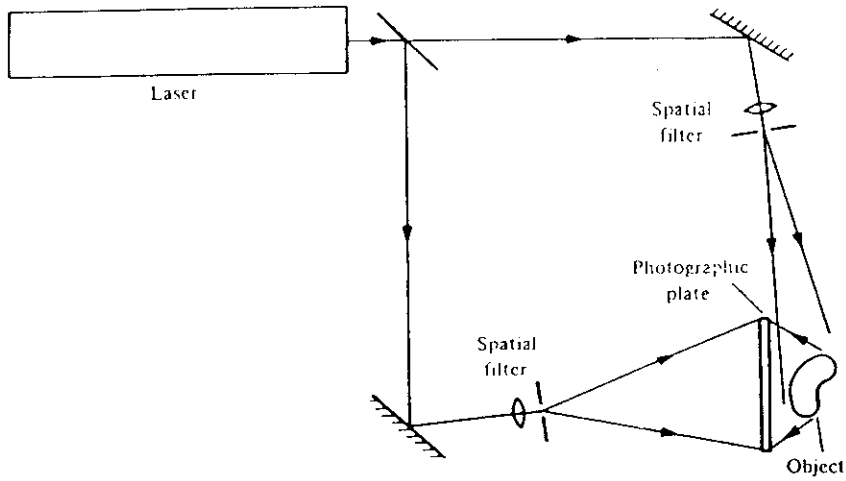

Fig. 10.2 Optical arrangement used to record a reflection hologram

10. Display holograms

A typical optical system for recording transmission holograms is shown in Fig.10.1. To avoid mechanical disturbances, all the optical components as well as the object and the photographic film or plate should be mounted on a stable surface resting on shock absorbers. The system is adjusted to have a low natural frequency of vibration (< 1 Hz). A concrete slab resting on inflated scooter inner tubes can be used, but most laboratories now use a honeycomb optical table with a metal top supported on pneumatic legs. The latter has the advantage that optical components can be bolted down to its surface or mounted on magnetic bases. The effects of air currents and acoustic disturbances can be minimized by enclosing the working area with heavy curtains.

Where very long exposures have to be made, residual disturbances can be eliminated by a feedback system which stabilizes the path difference between the beams [10.1]. Any motion of the fringes in the hologram plane is picked up by a photo detector, and variations in its output are amplified and applied to a PZT which controls the position of one of the mirrors in the beam path.

10.1 Reflection holograms

A typical optical system that can be used for recording reflection holograms is shown schematically in Fig.10.2. As can be seen, the

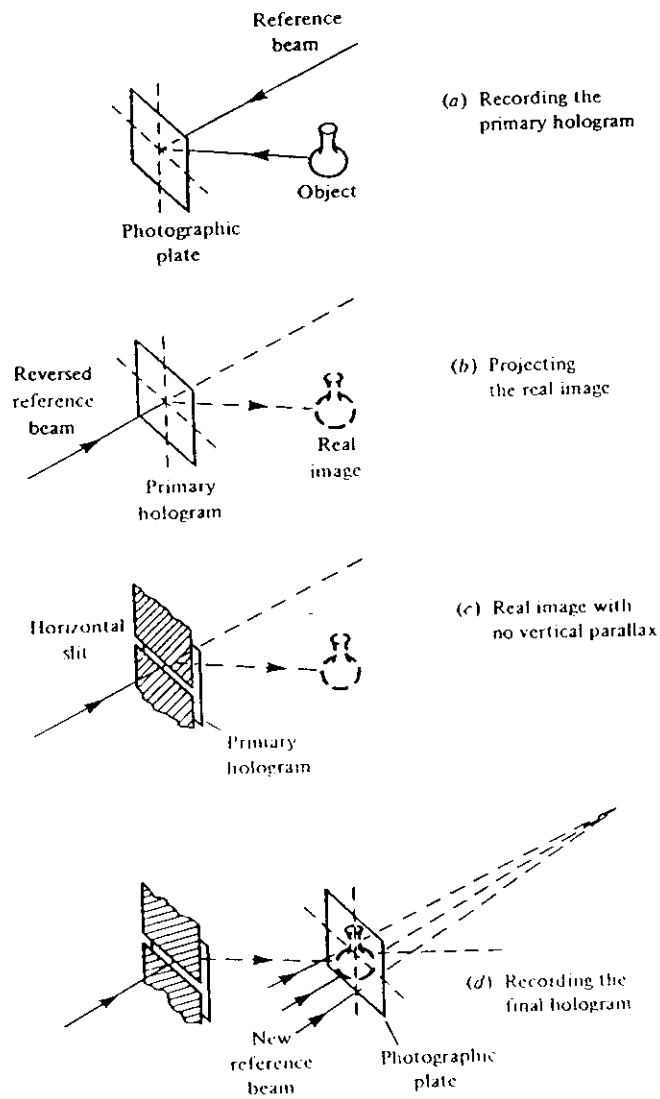

Fig. 10.3 Steps involved in the production of a rainbow hologram

object and reference waves are incident on the photographic emulsion from opposite sides. Since the thickness of the photographic emulsion is typically around 6 μm, the interference fringes are recorded as layers within it, about half a wavelength apart. The hologram exposure should be adjusted to give a density of about 2.0 after development, after which the hologram is processed in a rehalogenating bleach to control emulsion shrinkage and the resulting wavelength shift [10.2].

Reflection holograms of a flat, specular object, such as a coin, can be recorded by placing the photographic plate on the object, and illuminating it through the photographic plate.

10.2 Rainbow holograms

The rainbow hologram is a transmission hologram which reconstructs a bright, sharp, monochromatic image when illuminated with white light [10.3]. As shown schematically in Fig. 10.3(a), the first step in making a rainbow hologram is to record a conventional transmission hologram of the object. When this hologram (H_1) is illuminated, as shown in Fig. 10.3(b), by the conjugate of the original reference wave, it reconstructs the conjugate of the original object wave and produces a real image of the object with unit magnification.

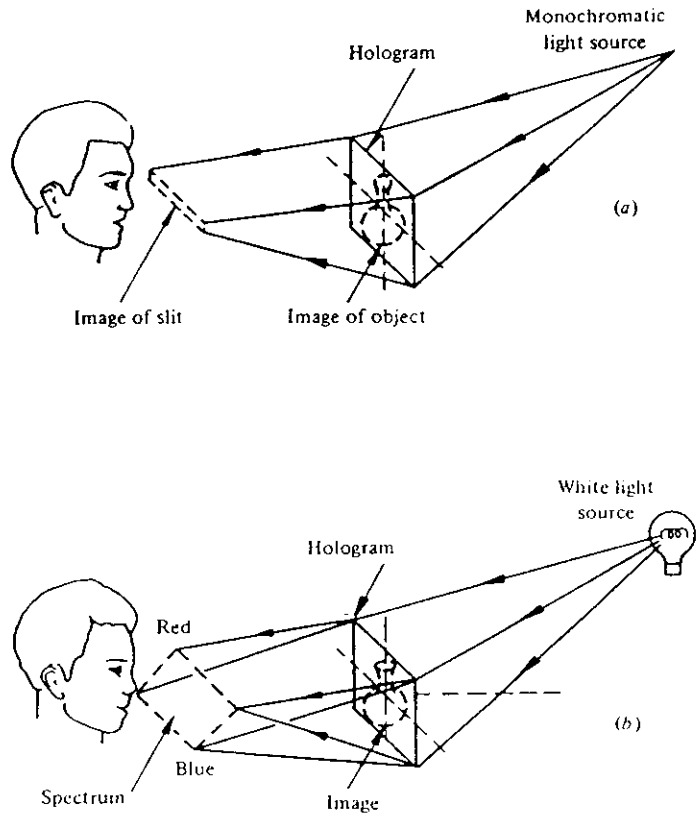

Fig. 10.4 Image reconstruction by a rainbow hologram (a) with monochromatic light and (b) with white light

A horizontal slit is then placed over H_1, as shown in Figs. 10.3(c) and 10.3(d), and a second hologram (H_2) is recorded of the real image produced by H_1. The reference beam for H_2 is a convergent beam inclined in the vertical plane, and the photographic plate used to record H_2 is placed so that the real image formed by H_1 straddles it.

When H_2 is illuminated with the conjugate of the reference beam used to make it, it forms an orthoscopic image of the object straddling the plane of the hologram, as shown in Fig. 10.4(a). In addition, it also forms a real image of the slit placed across H_1. All the light diffracted by the hologram passes through this slit pupil, so that a very bright image is seen from this position. Since the observer can move his head from side to side, horizontal parallax is retained. However, the image disappears if the observer's eyes move outside this slit pupil, so that vertical parallax is eliminated.

With a white-light source, the slit image is dispersed in the vertical plane, as shown in Fig. 10.4(b), to form a continuous spectrum. An observer whose eyes are positioned at any part of this spectrum then sees a sharp, three-dimensional image of the object in the corresponding colour.

Figure 10.5 shows an optical system that permits both steps of the recording process to be carried out with a minimum of adjustments. A collimated reference beam is used to record the primary hologram (H_1).

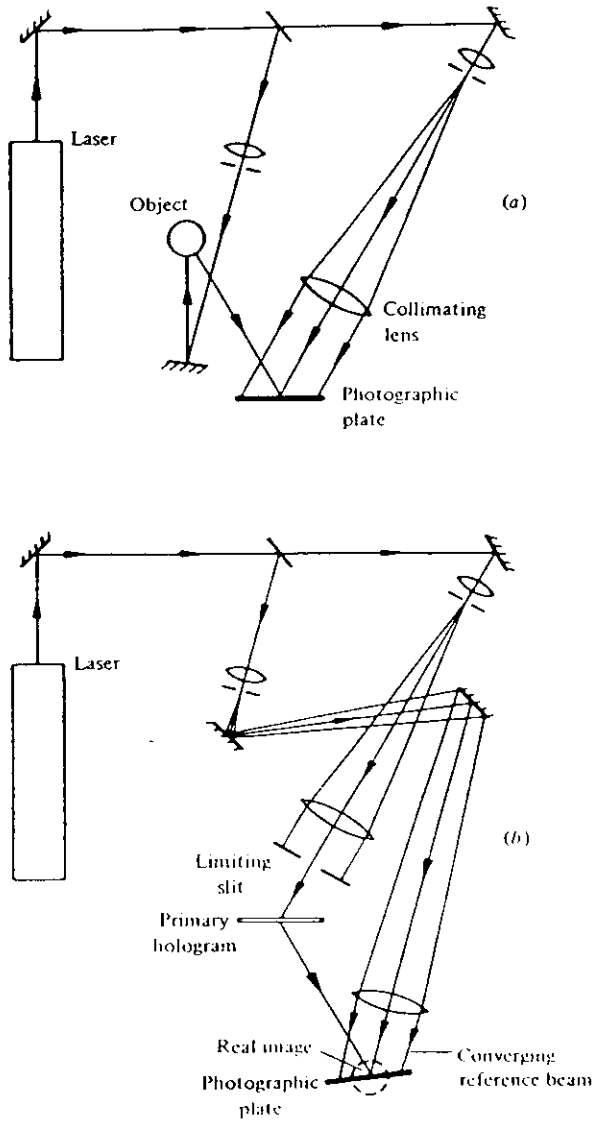

Fig. 10.5 Optical arrangement used to record a rainbow hologram

It is then necessary only to turn H_1 through 180^o about an axis normal to the plane of the figure and replace it in the holder. An undistorted real image is then projected into the space in front of H_1. Vertical parallax is eliminated by a slit a few millimetres wide placed over H_1 with its long dimension normal to the plane of the figure (This orientation corresponds to the horizontal in the final viewing geometry). A convergent reference beam is used to record the final hologram, which, after processing, is reversed for viewing. When H_2 is illuminated with a divergent beam from a point source of white light, an orthoscopic image of the object is formed, and a dispersed real image of the slit is projected into the viewing space.

10.3 Holographic stereograms

It is also possible to synthesize a hologram that reconstructs an acceptable three-dimensional image from a series of two-dimensional views of an object from different angles [10.4]. To produce such a holographic stereogram, a series of photographs of the subject is taken from equally spaced positions along a horizontal line. Alternatively, the subject can be placed on a slowly rotating turntable and a movie camera used to make a record of a 120^o or 360^o rotation. Typically, three movie frames are recorded for each degree of rotation [10.5].

The optical system used to produce a holographic stereogram from such a movie film is shown schematically in Fig. 10.6. Each frame is

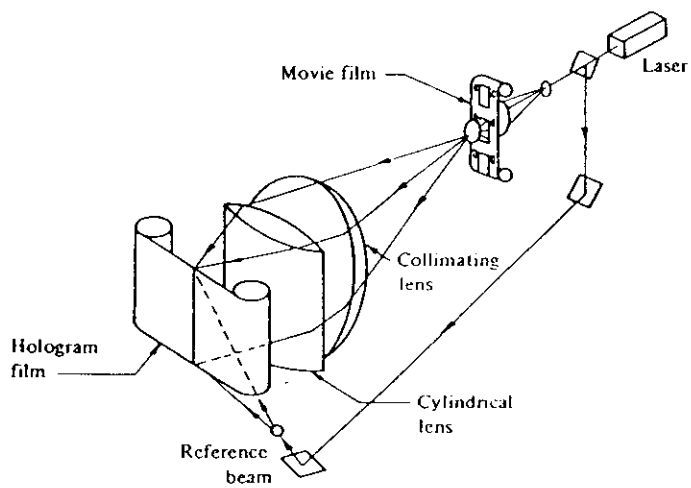

Fig. 10.6 Optical system used to produce a white-light holographic stereogram

imaged in the vertical plane on the film used to record the hologram. However, in the horizontal plane, the cylindrical lens brings the image to a line focus. A contiguous sequence of vertical strip holograms is recorded of successive movie frames, covering the full range of views of the original subject, using a reference beam incident at an appropriate angle either from above or from below. With a rotating subject, the processed film is formed into a cylinder for viewing.

When the holographic stereogram is illuminated with white light, the viewer sees a monochromatic three-dimensional image. This image changes colour, as with a rainbow hologram, when the observer moves his head up or down. The image lacks vertical parallax, but it exhibits horizontal parallax over the range of angles covered by the original photographs.

The obvious advantage of this technique, over recording a hologram directly, is that white light can be used to illuminate the subject in the first stage, so that holographic stereograms can be made of living subjects as well as large scenes. Some subject movement can also be displayed without destroying the stereoscopic effect.

10.4 Multicolour holograms

In principle, a multicolour image can be produced by a hologram recorded with three suitably chosen wavelengths, when it is illuminated

once again with these wavelengths. However, a problem is that each hologram diffracts, in addition to the wavelength used to record it, the other two wavelengths as well. The cross-talk images produced in this fashion overlap with and degrade the multicoloured image.

One way to eliminate cross-talk makes use of the high wavelength selectivity of volume reflection holograms. If such a hologram is recorded with three wavelengths, one set of fringe planes is produced for each wavelength. When the hologram is illuminated with white light, each set of fringe planes diffracts a narrow band of wavelengths centred on the original wavelength used to record it, giving a multicolour image free from cross-talk [10.6].

Improved diffraction efficiency can be obtained by superimposing three bleached volume reflection holograms recorded on two plates, one with optimum characteristics for the red, and the other with optimum characteristics for the green and blue. Brighter images can also be obtained if the final holograms are produced using a real image of the object projected by primary holograms whose aperture is limited by a suitably shaped stop [10.7].

Another method makes use of superimposed rainbow holograms [10.8] In this technique, three primary holograms are made with red, green and blue laser light. These primary holograms are then used with the same laser sources to make a set of three rainbow holograms, which are then

superimposed. When this multiplexed hologram is illuminated with a white light source, it reconstructs three images of the object. In addition, as shown in Fig. 10.7, three dispersed images of the slit are formed in the viewing space. These spectra are displaced with respect to each other, so that an observer, viewing the hologram from the original position of the slit, sees three superimposed images of the object reconstructed in the colours with which the primary holograms were made.

Multicolour rainbow holograms are very effective in displays since they reconstruct very bright images which exhibit high colour saturation and are free from cross-talk.

References

10.2 P. Hariharan and C. M. Chidley, Appl. Opt., 28, 422-424 (1989).

10.3 S. A. Benton in Applications of Holography and Optical Data Processing, eds. E. Marom, A. A. Friesem and E. Wiener-Avnear (Pergamon Press, Oxford) pp. 401-409.

10.4 J. T. McCrickerd and N. George, Appl. Phys. Lett. 12, 10-12 (1968).

10.5 S. A. Benton, Opt. Eng., 14, 402-407 (1975).

10.6 J. Upatnieks, J. Marks and R. Federowicz, Appl. Phys. Lett., 8, 286-287 (1966).

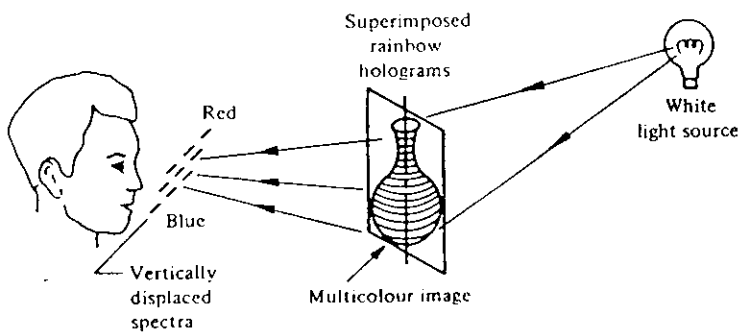

Fig. 10.7 Multicolour image reconstruction by superimposed rainbow holograms

10.7 P. Hariharan, J. Optics (Paris), 11, 53-55 (1980).

10.8 P. Hariharan, W. H. Steel and Z. S. Hegedus, Opt. Lett., 1, 8-9 (1977).

Problems

10.1 What is the theoretical improvement in diffraction efficiency possible in a multicolour hologram by recording the three component holograms on three separate plates instead of on a single plate?

If all the three holograms are recorded on a single photographic plate, the available dynamic range is divided between the three holograms (see Section 6.4). The diffraction efficiency of each component hologram is then only $(1/3)^2 = 1/9$ of that for a single hologram recorded on the same plate. The diffraction efficiency should therefore improve, theoretically, by a factor of 9 (the actual gain is about half this, because of transmission losses).

11. Particle imaging

A microscope which can resolve particles of diameter d has a depth of field

$$\Delta z = d^2 / 2\lambda \qquad (11.01)$$

Because of this limitation, measurements of the size of small particles distributed through an appreciable volume are not possible with a conventional imaging system. This problem can be overcome by using a hologram recorded with a pulsed laser to store a high-resolution, three-dimensional image of the whole field at any instant. The stationary image reconstructed by the hologram can then be examined in detail, throughout its volume, with a conventional microscope [11.1].

Wherever a sufficient amount of light (> 80 percent) is directly transmitted and can serve as a reference beam, it is possible to use in-line holography. This permits a very simple optical system, which is also economical of light. Because of the very small diameter of the particles, the distance z of the recording plane from the particles can be made to satisfy the far-field condition, $z >> d^2 / \lambda$, quite easily. The hologram formed in the far field of the particles by the interference of the diffracted light and the directly transmitted light is known as a Fraunhofer hologram.

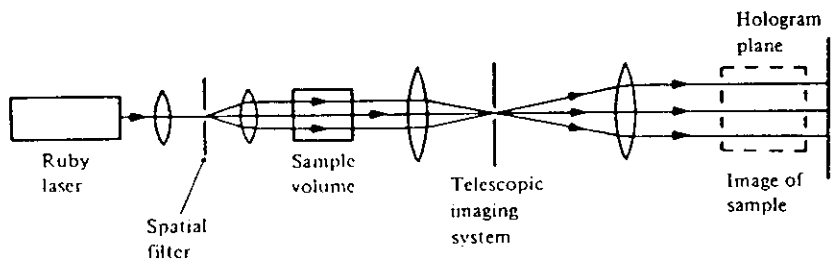

Fig. 11.1 In-line holographic system for particle-size analysis

The permissible exposure time for recording a hologram of a moving particle field depends on the velocity of the particles. For size analysis, a useful criterion is that the particle should not move by more than a tenth of its diameter during the exposure. Suitable light sources are either a pulsed ruby laser or, where a higher repetition rate is necessary, a frequency-doubled Nd:YAG laser.

To give an acceptable image of a particle, the hologram must record the central maximum and at least three side bands of its diffraction pattern. This would correspond to recording waves travelling at a maximum angle

$$\theta_{max} = 4\lambda \ / \ d \qquad (11.02)$$

to the directly transmitted wave, and, hence, to a maximum fringe frequency of $4 \ / \ d$, which is independent of the values of λ and z.

It also follows from Eq. (11.02) that for a given half-width of the hologram, x_{max}, the maximum depth of field over which the required resolution can be obtained is given by the relation

$$\Delta z_{max} = x_{max} d \ / \ 4\lambda. \qquad (11.03)$$

To view the image, the hologram is illuminated with a collimated beam of light from a He-Ne laser. With normal processing, negative

images are formed, but this is not a problem for most technical applications. Two images are formed at equal distances z from the hologram, one in front of it and the other behind it. However, with a Fraunhofer hologram, the contribution of the unwanted image in the plane of the primary image is esentially constant over the whole field. Accordingly, it does not degrade the primary image significantly.

Holographic particle size analysis has found several applications [11.2] including studies of fg droplets, dynamic aerosols and marine plankton. Another significant application has been in bubble-chamber photography. Double-exposure holography has been used to measure the velocity distribution of moving particles [11.3].

References

11.1 B. J. Thompson, J. Phys. E. 7, 781-788 (1974).

11.2 J. D. Trolinger, Opt. Eng., 14, 383-392 (1975).

11.3 B. C. R. Ewan, Appl. Opt., 18, 3156-3160 (1979).

Problems

11.1 Holographic imaging is to be used to study the size and spatial distribution of particles with diameters down to 10 μm, moving with velocities up to 1 m/s, in a field with a depth of 5 mm. Mechanical constraints require the hologram plate to be at a distance of 5 mm from the near side of the field. Determine (a) the minimum size of the hologram, (b) the minimum resolving power of the recording material, and (c) the maximum permissible exposure time.

The far side of the field is at a distance of 10 mm from the hologram. Accordingly, from Eq. (11.03) we require a hologram with a half-width

$$\begin{aligned} x_{max} &= z_{max}(4\lambda/d) \\ &= 10 \times 10^{-3} \times 4 \times 0.694 \times 10^{-6} \,/\, 10 \times 10^{-6} \text{ m} \\ &= 27.8 \text{ mm} \end{aligned}$$

From Eq. (11.02), the maximum fringe frequency to be recorded is 4/0.01 = 400 lines/mm. The resolving power of the film used must be greater than this value. During the exposure, a particle should not move by more than a tenth of its diameter. The maximum exposure time is, therefore, 1 μs.

12. Holographic optical elements

A hologram can be used to transform an optical wavefront in the same manner as a lens. However, holographic optical elements (HOEs) can also perform many unique functions and have been used in several specialized applications.

A major advantage of HOEs over conventional optical elements is that their function is independent of substrate geometry. In addition, since they can be produced on thin substrates, they are quite light, even for large apertures. Another advantage is that several holograms can be recorded in the same layer, so that spatially overlapping elements are possible. Finally, HOEs provide the possibility of correcting system aberrations in a single element, so that separate corrector elements are not required.

The recording material for a HOE must have high resolution, good stability, high diffraction efficiency and low scattering. Photo resists and dichromated gelatin are, at present, the most widely used materials. Photopolymers are an attractive alternative.

12.1 Diffraction gratings

High quality diffraction gratings can be produced by recording an interference pattern in a layer of photoresist coated on an optically

worked blank. The grating can be blazed to obtain maximum diffraction efficiency for a specified wavelength by setting the photoresist layer obliquely to the fringe pattern so as to generate a triangular groove profile [6.1]. After processing, the surface of the photoresist is coated with an evaporated metal layer.

12.2 Holographic scanners

Holographic scanners are significantly cheaper than mirror scanners and are widely used in point of sale terminals and for high-speed non-impact printing [12.2]. A typical scanner consists of a disc with a number of holograms recorded on it, with a point source as the object and a collimated reference beam. Rotating the disc causes the reconstructed image spot to scan the image plane.

With this simple arrangement, the scanning line is an arc of a circle with a radius

$$r = d \sin \theta \tan \theta, \qquad (12.01)$$

where d is the distance from the scanning facet to the centre of the image plane, and θ is the angle between the diffracted principal ray and the normal to the hologram.

A straight line scan can be obtained by using an auxiliary reflector to make the principal diffracted ray normal to the scanned surface, as shown in Fig. 12.01. This system is also self-compensating for wobble of the scanning disc when $\theta_i = \theta_d = 45^o$.

12.3 Aberration correction

Computer-generated holograms are now used widely in interferometric tests of aspheric surfaces, where they replace expensive null lenses previously used to cancel the aberrations of the test wavefront [12.3]. The hologram is a representation of the interferogram that would be obtained if the wavefront from the desired aspheric surface were to interfere with a tilted plane wavefront. If the test surface is imaged on the hologram, the superposition of the actual interference pattern and the hologram produces a moire pattern showing the deviation of the test wavefront from the ideal computed wavefront.

12.4 Head-up displays

One of the most successful applications of HOEs has been in head-up displays for high-performance aircraft, where, as shown in Fig. 12.2, they project an image of the instruments at infinity, along the pilot's normal line of vision [12.4]. Holographic optical elements are lighter and can be fitted into the limited space available. In addition,

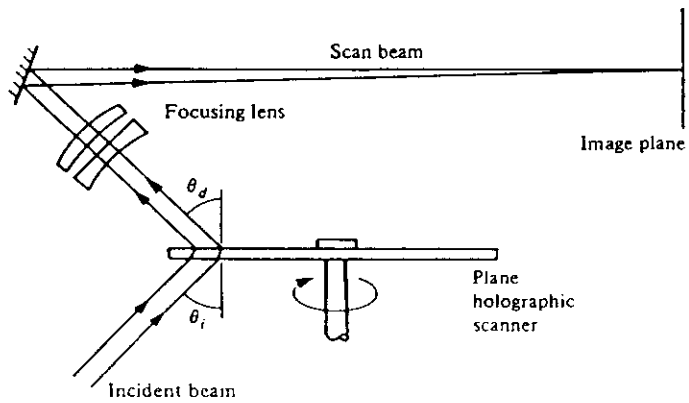

Fig. 12.1 Plane-grating holographic scanner giving a straight-line scan

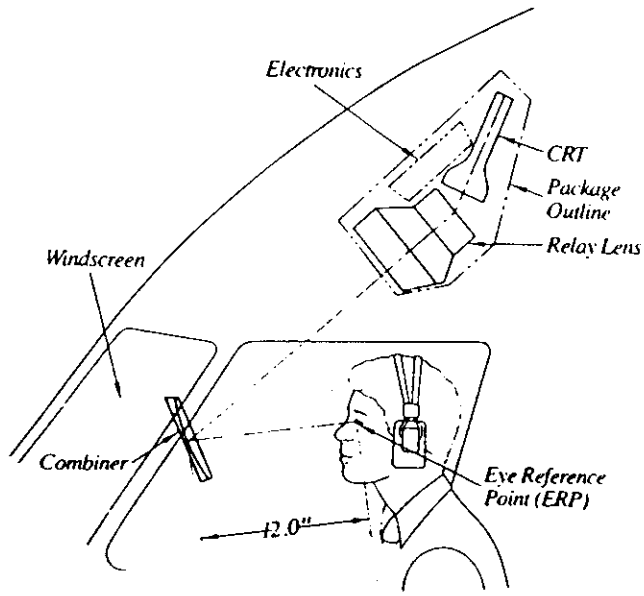

Fig. 12.2 Optical system used in an aircraft head-up display

reflection holograms can be made with a high reflectance over a narrow band of wavelengths and high transmission at all other wavelengths.

12.5 Multiple imaging

There are many applications where it is necessary to produce an array of identical images. Holographic elements can be used to produce such an array with a single exposure [12.5].

The optical system used is shown in Fig. 12.3. The object transparency, whose amplitude transmittance is $f(x,y)$, is placed in the front focal plane of the lens L_1 and illuminated by a collimated beam. The Fourier transform of this object, $F(\xi,\eta)$, is then displayed in the back focal plane of L_1.

To generate an $n \times m$ array of images separated by intervals x_0, y_0, a hologram with an amplitude transmittance

$$H(\xi,\eta) = \sum^{n} \sum^{m} \exp\left[-\, i2\pi\, (nx_0\xi + my_0\eta)\right] \qquad (12.02)$$

is placed in the back focal plane of the lens L_1. The wavefront emerging from this hologram can be written as

$$G(\xi,\eta) = F(\xi,\eta)\; H(\xi,\eta). \qquad (12.03)$$

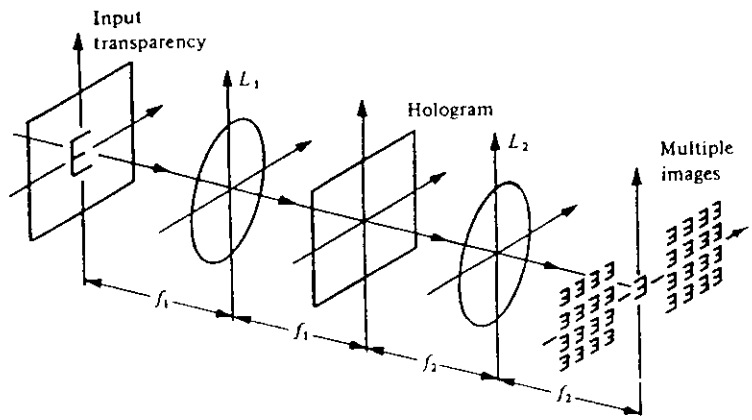

Fig. 12.3 Generation of multiple images by a hologram

A second Fourier transform operation by the lens L_2 then produces a set of multiple images

$$g(x,y) = f(x,y) * \sum_{n}\sum_{m} \delta(x - nx_0,\ y - my_0),$$
$$= \sum_{n}\sum_{m} f(x - nx_0,\ y - my_0). \qquad (12.04)$$

12.6 Interconnections

Integrated circuits in a computer are traditionally connected by metallic wires. However, such connections have several drawbacks at high data rates. One way to overcome these problems is the use of optical interconnections [12.6].

Many interconnection networks rely on one-to-one interconnects between an input array and an output array, and can be described by a permutation matrix. As shown in the previous section, a HOE can be used to redirect light from each laser source of the input array to one or more detectors of the output array. A particularly interesting possibility is the use of dynamic holograms recorded in a photorefractive crystal to generate new input-output configurations in a switching network [12.7].

References

12.1 M. C. Hutley, J. Phys. E: Sci. Instrum., 9, 513-520 (1976).

12.2 L. Beiser, Holographic Scanning (Wiley, New York, 1988).

12.3 J. C. Wyant and V. P. Bennett, Appl. Opt. 11, 2833-2839 (1972).

12.4 D.G. McCauley, C. E. Simpson and W. J. Murbach, Appl. Opt. 12, 232-242 (1973).

12.5 S.Lu, Proc. IEEE, 56, 116-117 (1968).

12.6 J. W. Goodman, F. J. Leonberger, S-Y. Kung and R. A. Athale, Proc. IEEE, 72, 850-866 (1984)

12.7 P.Yeh, A. E. T. Chiou and J.Hong, Appl. Opt. 27, 2093-2096 (1988).

13. Holographic interferometry

In holographic interferometry, at least one of the interfering waves is reconstructed by a hologram. Its major attraction is the fact that holography makes it possible to store a wavefront and reconstruct it at a later time. As a result, interferometric techniques can be used to compare two wavefronts which were originally separated in time or space, or even wavefronts of different wavelengths. In addition, since a hologram reconstructs the shape of an object with a rough surface faithfully, down to its smallest details, large scale changes in ~~its~~ the shape of almost any object can be measured with interferometric precision [13.1-13.4].

Equations (4.01- 4.04) show that if a hologram is replaced in its original position in the same setup used to record it, and illuminated with the original reference wave, it reconstructs the original object wave. If, then, the shape of the object changes slightly, the directly transmitted object wave will interfere with the reconstructed object wave to produce, as shown in Fig. 13.1, a fringe pattern that maps the changes in the shape of the object.

13.1 Real-time holographic interferometry

If the changes in the shape of the object are small, only the phase of the object wave is modified, and the complex amplitude of the wave from the deformed object can be written as

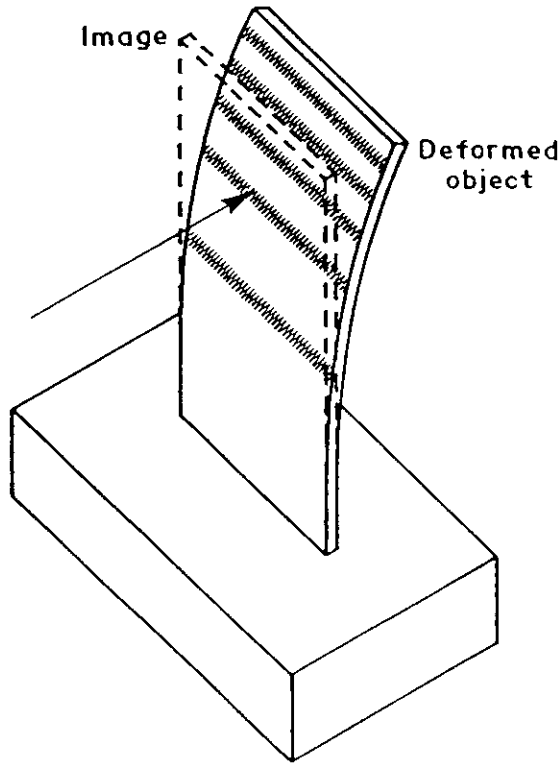

Fig. 13.1 Generation of holographic interference fringes by deformation of an object.

$$o'(x,y) = o(x,y) \exp [-i\Delta\varphi(x,y)] \qquad (13.01)$$

where $o(x,y)$ is the complex amplitude of the original object wave, and $\Delta\varphi(x,y)$ is the phase change arising from the deformation. Accordingly, from Eq. (3.06), the complex amplitude of the directly transmitted object wave is

$$u_1(x,y) = (t_0 + \beta Tr^2)\, o'(x,y), \qquad (13.02)$$

while the complex amplitude of the reconstructed object wave is

$$u_2(x,y) = \beta Tr^2\, o(x,y). \qquad (13.03)$$

The intensity in the interference pattern produced by these two waves is, therefore,

$$\begin{aligned} I(x,y) &= |u_1(x,y) + u_2(x,y)|^2 \\ &= |o(x,y)|^2 [A^2 + (t_0 - A)^2 - 2A(t_0 - A) \cos \Delta\varphi(x,)], \end{aligned} \qquad (13.04)$$

where $A = -\beta Tr^2$. Since β is negative, dark fringes are seen when $\Delta\varphi(x,y) = m\pi$, where m is an integer.

Interference fringes obtained by this technique can be used to study changes in the shape of the object in real time. The problem of

replacing the hologram in its original position can be eliminated by in situ processing of the hologram plate, or by using a photothermoplastic or a photorefractive crystal as the recording material.

13.2 Double-exposure holographic interferometry

It is also possible to record two holograms on the same photographic plate; one of the object in its original state, and the other of the deformed object. The resultant complex amplitude, due to the superposition of the two reconstructed images is then, apart from a constant of proportionality,

$$\begin{aligned} u(x,y) &= o(x,y) + o'(x,y) \\ &= o(x,y)\ \{1 + \exp\ [-i\Delta\varphi(x,y)]\}. \end{aligned} \tag{13.05}$$

and the intensity in the image is

$$I(x,y) = |o(x,y)|^2\ [1 + \cos\ \Delta\varphi(x,y)]. \tag{13.06}$$

In this case, bright fringes are seen when $\Delta\varphi(x,y) = 2m\pi$.

This technique has the advantage that repositioning of the hologram is not critical, since the two interfering waves are always reconstructed in exact register. In addition, the visibility of the fringes is always good, since the two waves have the same polarization

and the same amplitude. With a pulsed laser, double-exposure holographic interferometry can be used to study transient phenomena.

A common problem in double-exposure holographic interferometry with a cw laser is unwanted object movements. Some types of object motion can be eliminated by reflecting the reference beam from a mirror attached to the object [13.5]. Alternatively, the hologram plate can be attached to the object, and a doubly-exposed reflection hologram can be recorded with the object illuminated through the hologram plate [13.6].

Another disadvantage is that information on intermediate states of the object is not available. This problem can be overcome by making a series of exposures at successive stages of loading, using a set of masks with apertures that overlap in a predetermined order [13.7]. The reconstructed images then yield interference patterns corresponding to any two stages of loading. Another way to overcome this problem is the sandwich hologram [13.8]. In this technique, pairs of photographic plates are exposed in the same plate-holder with their emulsion-coated surfaces facing the object. One pair is exposed with the unstressed object, and successive pairs are exposed at different stages of loading. The back plate from the first pair can then be put together with the front plate from any other pair to produce an interference pattern showing the surface deformation at this stage. In addition, ambiguities

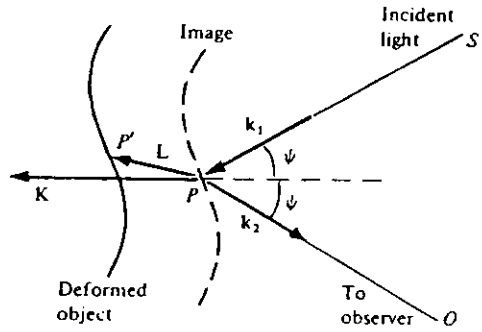

Fig. 13.2 Evaluation of the phase difference produced by a local displacement of the object

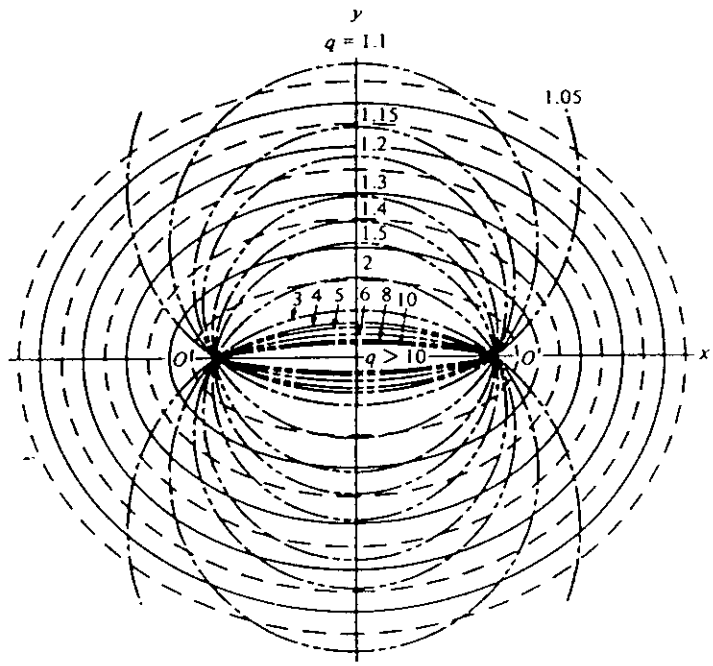

Fig. 13.3 The holodiagram. The ellipses are loci of constant path length; the circles are loci of constant K [Abramson, 1969]

can be resolved by tilting the sandwich; this is equivalent to tilting the object between the two exposures.

13.3 Phase difference in the interference pattern

With an object having a rough surface, the phase varies in a random manner across the object wavefront. As a result, only waves from corresponding points on the object wavefront and the reconstructed wavefront contribute effectively to the interference pattern, and the intensity at any point in it is determined by the phase difference between the waves from these two points.

To evaluate this phase difference, we consider a point P on the surface which, as shown in Fig. 13.2, has undergone a vector displacement L to P′. If the displacement of P is small compared to the distances to the source S and the point of observation O, the phase difference introduced is

$$\begin{aligned} \Delta\varphi &= \mathbf{L}\cdot(\mathbf{k}_1 - \mathbf{k}_2) \\ &= \mathbf{L}\cdot\mathbf{K}, \end{aligned} \qquad (13.07)$$

where $\mathbf{k}_1$ and $\mathbf{k}_2$ are the propagation vectors of the incident and scattered beams, and $\mathbf{K} = \mathbf{k}_1 - \mathbf{k}_2$ is known as the sensitivity vector [13.9 - 13.11].

13.4 The holodiagram

The holodiagram is a useful aid to interpretation of the interference fringes [13.12]. As shown in Fig. 13.3, the holodiagram consists of a set of ellipses whose foci, O and O′, correspond to the beam splitter and the viewing point on the photographic plate, respectively, in the recording system. For any object point P, the ellipse on which it lies is the locus for which the distance OPO′ is a constant. A displacement of P from one ellipse to the next corresponds to a change in this distance of one wavelength and a shift of one fringe in the interference pattern. The required displacement of P is obviously a minimum when its motion is along the normal to the ellipse, which corresponds to the sensitivity vector K.

The circles drawn through O and O′ are curves of constant K. They correspond to the specified values of the parameter $q = 1 / \cos \psi$, where the angle $OPO' = 2\psi$. These curves can be used to optimize a hologram recording system for a particular type of surface displacement.

13.5 Fringe localization

With an object having a rough surface, the visibility of the interference fringes is a maximum for a particular position of the plane of observation, known as the plane of localization.

As mentioned earlier, because of the random phase variations across the object wavefront, only waves from corresponding points on the two interfering wavefronts contribute effectively to the interference fringes. For a given viewing direction, the phase difference $\Delta\varphi$ between the waves from two such points, P and P′ (see Fig. 13.2), is defined by Eq.(13.07). In general, this phase difference will vary over the range of viewing directions defined by the aperture of the viewing lens, resulting in a loss of contrast of the fringes. However, it is possible to find a plane in which the value of $\Delta\varphi$ is very nearly constant over this range of viewing directions; this is the plane of localization of the fringes [13.13].

The position of the plane of localization depends on the type of displacement. Two cases are of particular interest. One is pure translation of the object, which produces fringes localized at infinity; the other is rotation of the object about an axis contained in its surface, which results in fringes localized at the surface [13.14, 13.15].

13.6 Stroboscopic holographic interferometry

Stroboscopic holographic interferometry can be used to map the amplitude of vibration of the surface of an object. In this technique, a hologram of the vibrating object is recorded using a sequence of light pulses that are triggered at times Δt_1 and Δt_2 after the start of each

vibration cycle. If the displacement of a point (x,y) on the object at time t is given by the relation

$$L(x,y,t) = L(x,y) \sin \omega t \qquad (13.08)$$

the intensity in the reconstructed image is

$$I(x,y) = I_0(x,y) \{1 + \cos [K \cdot L(x,y) (\sin \omega t_1 - \sin \omega t_2)]\}. \qquad (13.09)$$

The hologram is equivalent to a double-exposure hologram recorded with the object in these two states of deformation.

13.7 Time-average holographic interferometry

In this technique a hologram is recorded of the vibrating surface with an exposure time which is long compared to the period of vibration [13.16]. The amount by which the phase of the light from any point on the object is shifted is then a function of time and can be written as

$$\Delta\varphi(x,y,t) = K \cdot L(x,y) \sin \omega t. \qquad (13.10)$$

The complex amplitude of the scattered light wave from the vibrating object can therefore be written as

$$o(x,y,t) = |o(x,y)| \exp \{-i[\varphi(x,y) + K \cdot L(x,y) \sin \omega t]\}. \qquad (13.11)$$

If the holographic recording process is linear, the complex amplitude u(x,y) of the wave reconstructed by the hologram will be proportional to the time-average of o(x,y,t) over the exposure interval T, so that we can write

$$u(x,y) = \frac{1}{T}\int_0^T |o(x,y)| \exp\{-i[\varphi(x,y) + K\cdot L(x,y)\sin\omega t]\}\,dt,$$

$$= |o(x,y)| \exp[-i[\varphi(x,y)]\frac{1}{T}\int_0^T \exp[-i\,K\cdot L(x,y)\sin\omega t]\,dt,$$

$$= o(x,y)\,M_T(x,y), \qquad (13.12)$$

where $M_T(x,y)$ is known as the characteristic function. If the exposure time is long compared to the period of the vibration ($T >> 2\pi/\omega$), we have

$$M_T(x,y) = \lim_{T\to\infty}\frac{1}{T}\int_0^T \exp[-i\,K\cdot L(x,y)\sin\omega t]\,dt,$$

$$= J_0[K\cdot L(x,y)], \qquad (13.13)$$

where J_0 is the zero-order Bessel function of the first kind. The intensity in the reconstructed image is then

$$I(x,y) = |o(x,y)M_T(x,y)|^2,$$

$$= I_0(x,y)\,J_0^2[K\cdot L(x,y)], \qquad (13.14)$$

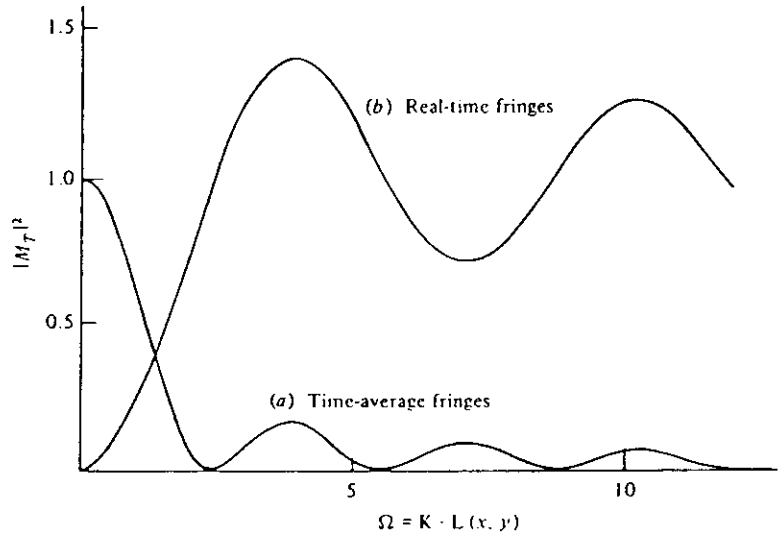

Fig. 13.4 Characteristic function for time-average fringes for a vibrating object

where $I_0(x,y)$ is the intensity in the image when the object is at rest.

The function $|M_T|^2$ is plotted against the parameter $\Omega = \mathbf{K}\cdot\mathbf{L}$ in Fig. 13.4. If the vibration amplitude varies over the object, Eq. (13.14) gives rise to fringes (contours of equal vibration amplitude) covering the reconstructed image. The dark fringes, at which the intensity drops to zero, correspond to the zeros of the function $J_0^2(\Omega)$, and the bright fringes to its maxima. The first maximum, which corresponds to the nodes, is the brightest, while the intensities of successive maxima, occurring at larger vibration amplitudes, fall off progressively.

Time-average holographic interferometry is a simple technique that permits ready identification of the vibration modes of an object, as well as accurate measurements of the vibration amplitudes. A typical series of interferograms obtained with an acoustic guitar, showing the resonant modes of its sound board, is presented in Fig. 13.5.

References

13.1 R. E. Brooks, L. O. Heflinger, R.F. Wuerker: Appl. Phys. Lett. 7, 248-249 (1965)

13.2 J. M. Burch, Prodn. Engineer: 44, 431-442 (1965)

13.3 R. J. Collier, E. T. Doherty, K. S. Pennington: Appl. Phys. Lett. 7, 223-225 (1965)

13.4 K. A. Haines, B. P. Hildebrand: Phys. Lett. 19, 10-11 (1965)

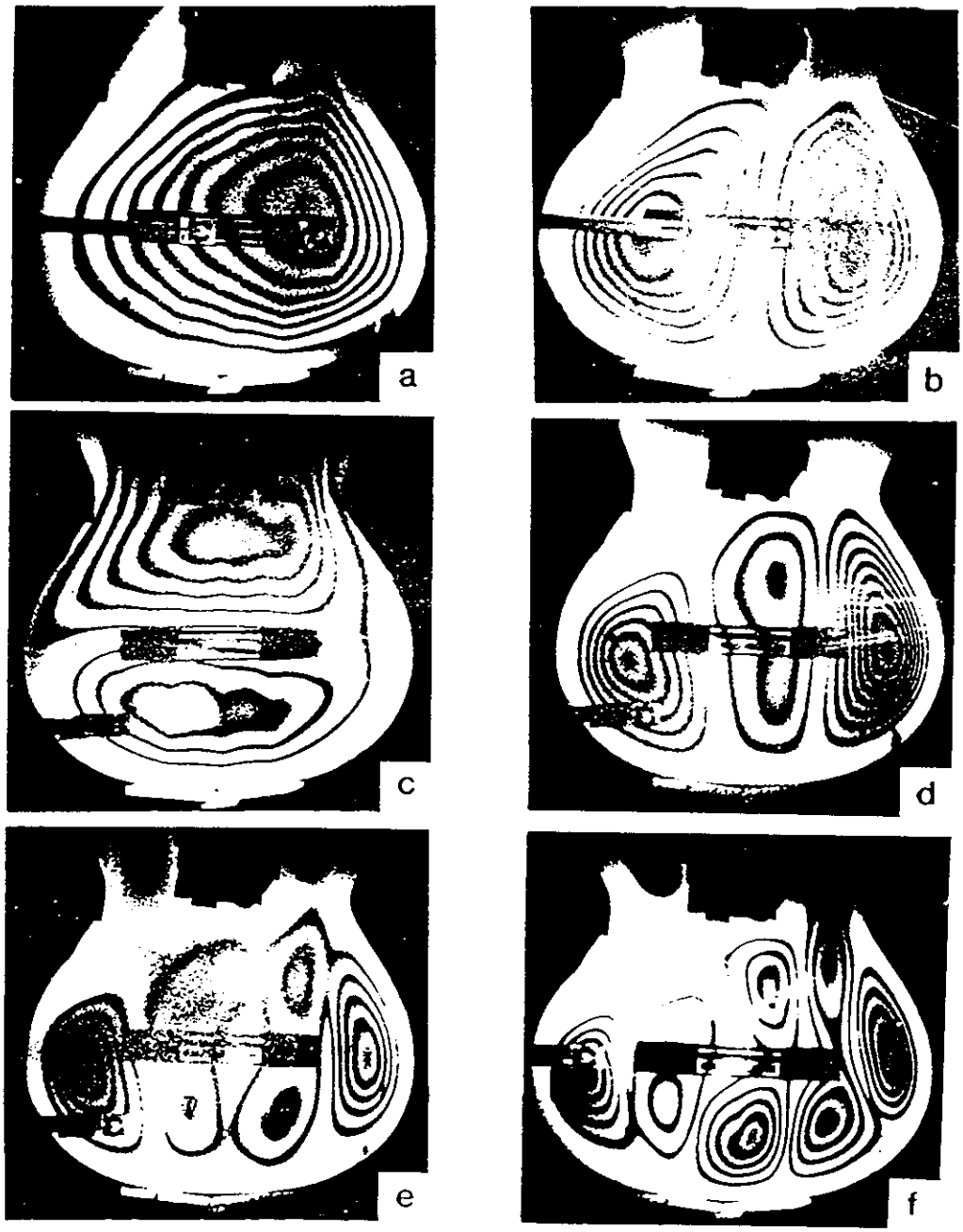

Fig. 13.5 Time-average holographic interferograms of the resonant modes of the soundboard of a guitar at frequencies of (a) 195, (b) 292, (c) 385, (d) 537, (e) 709 and (f) 905 Hz.

13.5 F. M. Mottier: Appl. Phys. Lett. **15**, 44-45 (1969)

13.6 P. M. Boone: Opt. Acta **22**, 579-589 (1975)

13.7 P. Hariharan, Z.S. Hegedus: Opt. Commun. **9**, 152-155 (1973)

13.8 N. Abramson: Appl. Opt. **13**, 2019-2025 (1974)

13.9 E. G. Aleksandrov, A. M. Bonch-Bruevich: Sov. Phys: Tech. Phys. **12**, 258-265 (1967)

13.10 A. E. Ennos: J. Phys. E: Sci. Instrum. **1**, 731-734 (1968)

13.11 J. E. Sollid: Appl. Opt. **8**, 1587-1595 (1969)

13.12 N. Abramson: Appl. Opt. **8**, 1235-1240 (1969)

13.13 S. Walles: Arkiv for Fysik **40**, 299-403 (1969)

13.14 N. E. Molin and K. A. Stetson, Optik **31**, 157-177 (1970)

13.15 N. E. Molin and K. A. Stetson, Optik **31**, 281-291 (1970)

13.16 R. L. Powell, K. A. Stetson: J. Opt. Soc. Am. **55**, 1593-1598 (1965)

Problems

13.1 A hologram is recorded of a circular diaphragm clamped by its edge over an opening in a pressure vessel and illuminated at 45^{o} with a beam from a He-Ne laser (λ = 633 nm). The hologram is viewed in a direction normal to the surface of the diaphragm. When the pressure in the vessel is increased slightly, four concentric circular fringes are seen covering the reconstructed image. What is the deflection of the centre of the diaphragm?

Since the edge of the diaphragm is fixed, and we have four fringes from the centre to the edge, the phase difference at the centre is

$$\Delta\varphi = 8\pi = 25.13.$$

We also know that the displacement of the centre of the diaphragm must be along the normal to its surface. Accordingly, it follows from Fig. 13.2 and Eq. (13.07) that the sensitivity vector

$$\begin{aligned} K &= (2\pi/\lambda)(1 + \cos 45^{o}) \\ &= 16.94 \times 10^{6}\ m^{-1}. \end{aligned}$$

The displacement of the centre of the diaphragm is therefore

$$\begin{aligned} L(0,0) &= \Delta\varphi/K \\ &= 25.13 \,/\, 16.94 \times 10^{6}\ m \\ &= 1.48\ \mu m. \end{aligned}$$

13.2 If the time-average holograms of the guitar in Fig. 13.5 have been recorded with the same setup as that described for Problem 13.1, what would be the vibration amplitudes of the soundboard in the resonant modes at 195 and 292 Hz?

In these two modes we have 7 and 6 dark fringes, respectively, from the edge of the soundboard to the point vibrating with the largest amplitude. Since the edge is at rest, the amplitudes of vibration at these points correspond (see Eq. 13.14) to the sixth and seventh zeros of the function J_0 (Ω), where $\Omega(x,y) = K \cdot L(x,y)$. Accordingly, we have

$$\Omega_{195} = 21.21$$
$$\Omega_{292} = 18.07.$$

The corresponding values of the vibration amplitude are, therefore

$$L_{195} = 21.21 \;/\; 16.94 \times 10^6 \text{ m}$$
$$= 1.25 \;\mu\text{m}.$$
$$L_{292} = 18.07 \;/\; 16.94 \times 10^6 \text{ m}$$
$$= 1.07 \;\mu\text{m}.$$

Note that for the mode at 292 Hz, a section of the soundboard between the two peaks is at rest; the displacements of the two peaks are therefore in opposite senses.